Single top s-channel cross section measurement with the ATLAS detector

Caterina Monini

Supervisors: Annick Lleres, Arnaud Lucotte

Ph.D. defense
Grenoble 12/09/2014

Outline

- Theoretical framework and analysis motivations
- Experimental approach
- s-channel cross section measurement
- Conclusion

Standard Model

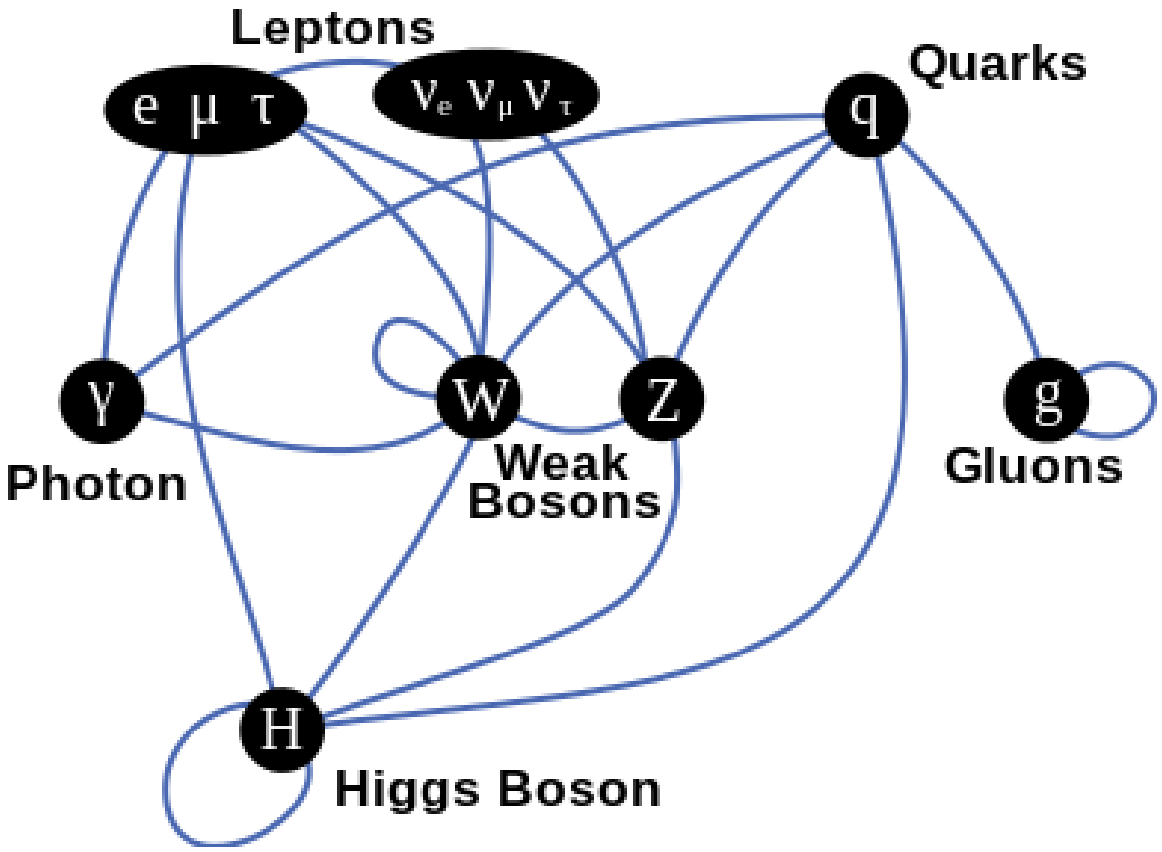

Renormalizable quantum field theory describing the fundamental forces and the elementary structure of matter

Top quark in SM

- Predicted in the 70's as weak isospin partner of the bottom quark
- Discovered in 1995 @ TeVatron

- Heaviest SM fermion:
  m(t)=173 ± 0.9 GeV (Phys. Rev. D 86, 2012)

  - peculiar role in the EWSB mechanism?
  - strong coupling to the Higgs

- Lifetime $\tau = 4 \cdot 10^{-25}$ s $< \tau_{QCD}$

  - It decays before hadronizing
  - Its polarization can be assessed from the decay products

- Decay proceeds almost exclusively via a bottom quark and W boson, it can be hadronic or semileptonic:

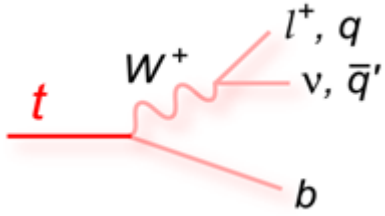

Top quark production @ LHC

via strong interaction: top pair

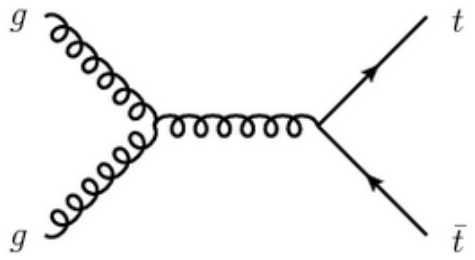

Gluon-gluon fusion

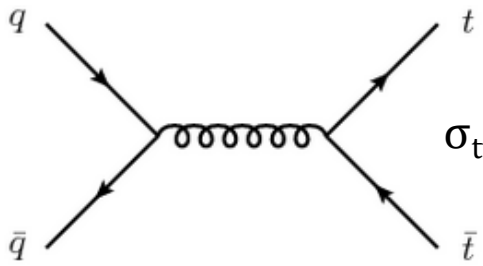

Quark antiquark annihilation

σ_{ttbar} at 8 TeV ≈253 pb

via electroweak interaction: single top

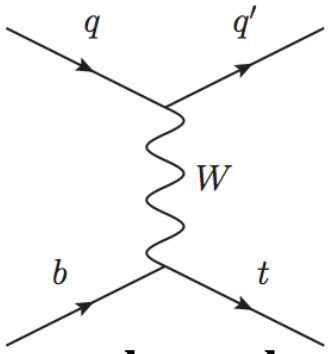

t-channel

observation 2010, DO

σ_t at 8 TeV ≈88 pb

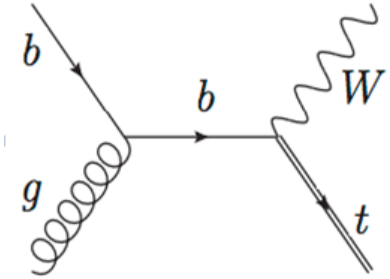

Wt-associated production

evidence 2012, ATLAS

observation 2013, CMS

σ_{Wt} at 8 TeV ≈22 pb

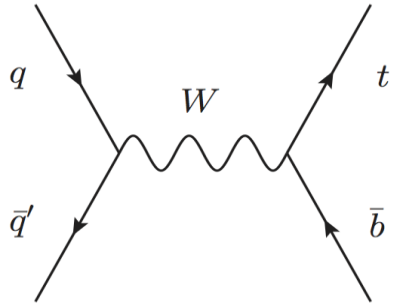

s-channel

observation 2014, D0 & CDF

σ_s at 8 TeV ≈6 pb

Single top measurements motivation

- **Constraints on the Cabibbo Kobayashi Maskawa matrix**

V_{tb} determination:

- Indirect measurements
- Top pairs decay,
  with the hypothesis of CKM unitarity

$$R = \frac{\mathcal{B}t \to Wb}{\mathcal{B}t \to Wq} = \frac{|V_{tb}|^2}{\sum_{q=1}^{3} |V_{tq}|^2} = |V_{tb}|^2$$

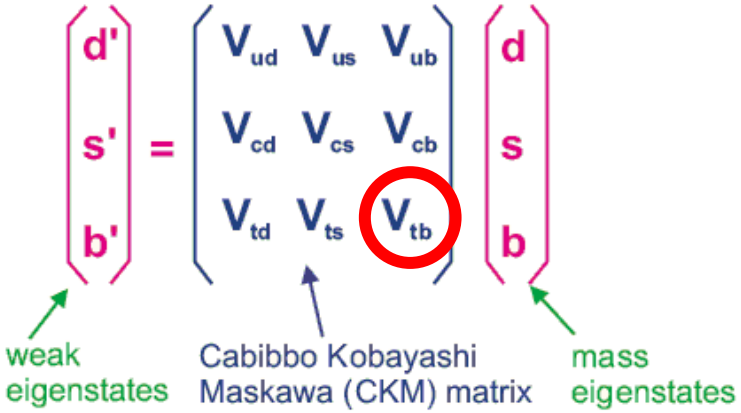

- Single top production,
  assuming left-handed coupling and $V_{tb} \gg V_{ts}, V_{td}$

$$|V_{tb}|^2 = \frac{\sigma^{exp}_{single\ top}}{\sigma^{th}_{single\ top}}.$$

- Single top production,
  model independent extraction of $|V_{tq}|$

Eur Phys J. C 72, 2012

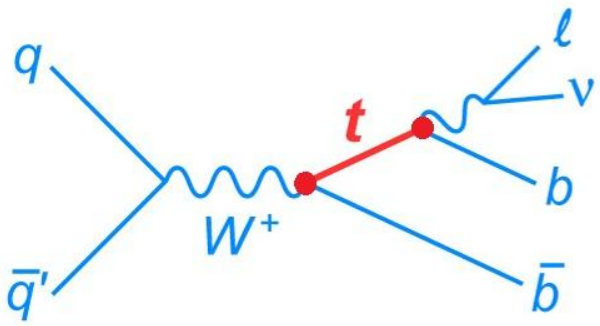

Single top measurements motivation

- **Sensitivity of beyond standard model (BSM) physics**

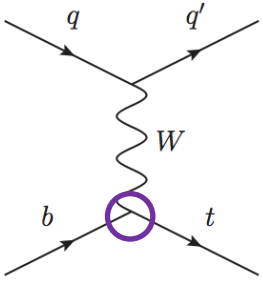

Anomalous couplings → modification of the W-t-b vertex
i.e Flavour Changing Neutral Currents
predicted at detectable rate by MSSM, ~~R~~ SUSY,
Top color assisted technicolor ...

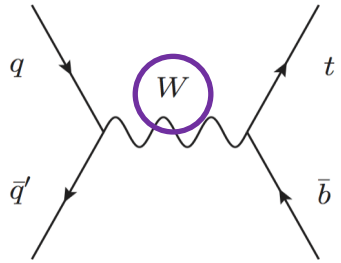

Extra gauge or scalar bosons produced as resonances or replacing the standard mediator
i.e. W', $H^{\pm}$ introduced by top flavour model, MSSM...
Direct production of "down" extra quarks

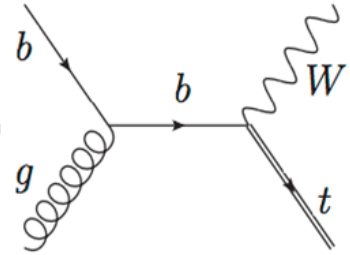

Smaller influence of new physics scenarios,
reference for SM physics

Interest of single top measurements

Single top channels : different sensitivities to new physics scenarios
→ combined constraints on several SM extensions

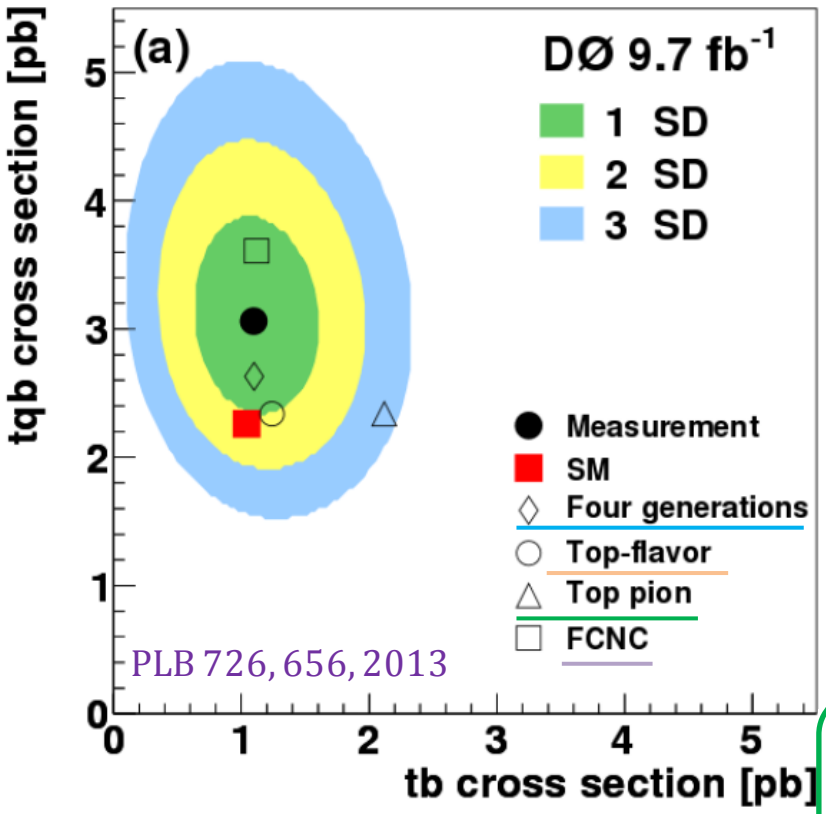

Analogous synthesis @ LHC
- t-channel: obbserved ($\Delta\sigma/\sigma < 20\%$)
- Wt-production: observed ($\Delta\sigma/\sigma \approx 23\%$)
- s-channel: no evidence yet

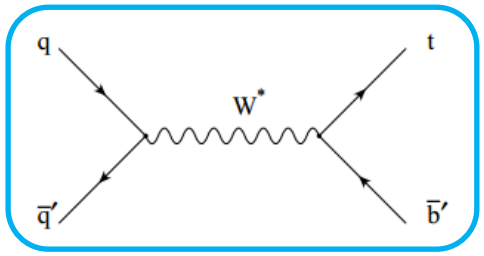

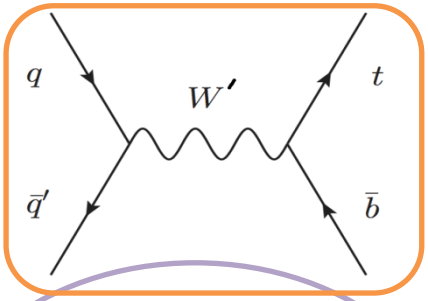

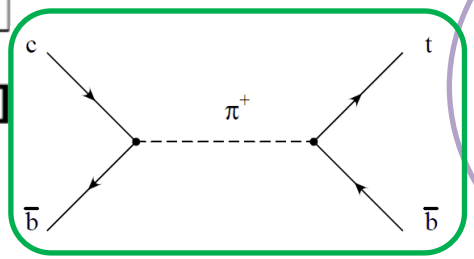

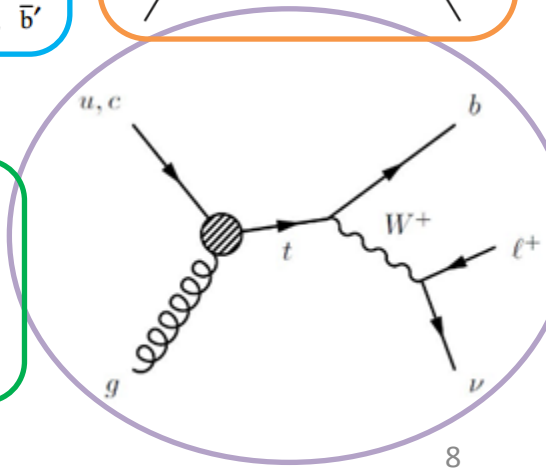

The LHC

Large Hadron Collider

designed for proton-proton collisions at a center of mass energy √s=14 TeV

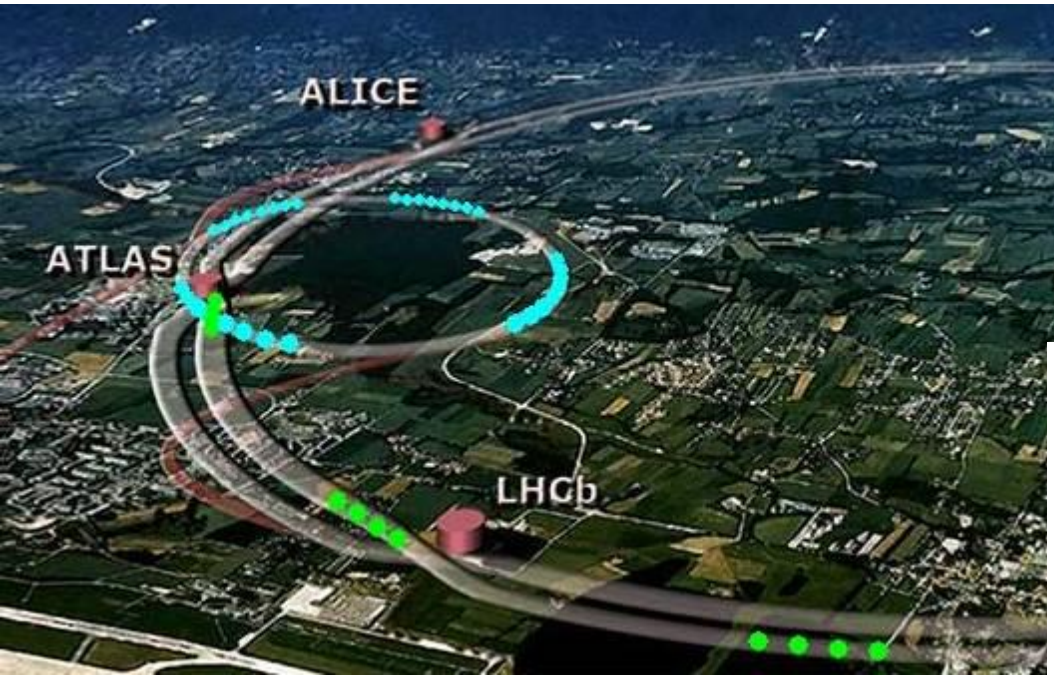

and heavy ions collisions

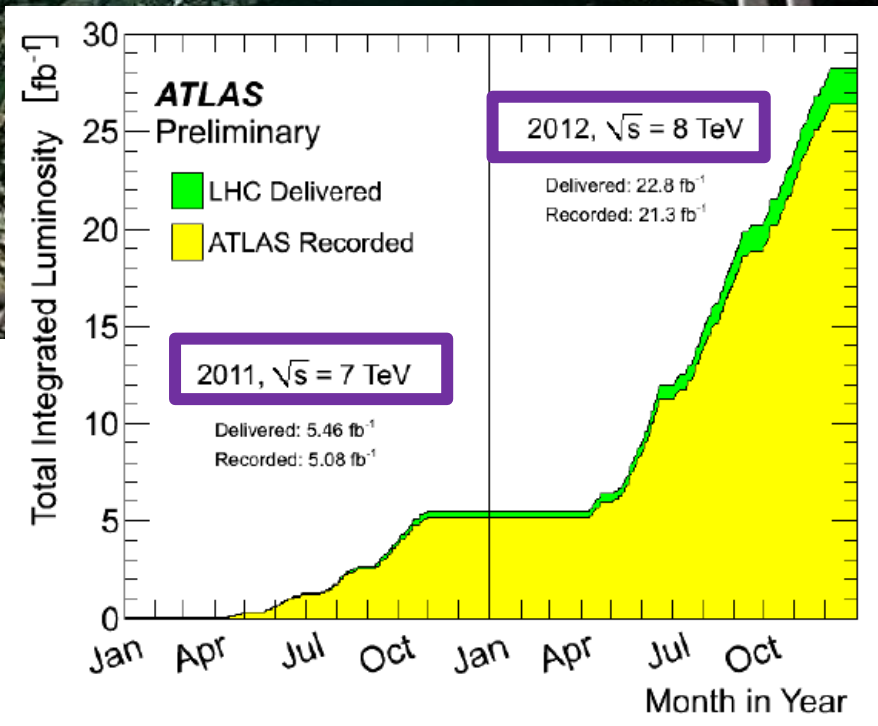

The ATLAS detector

Single top s-channel final state

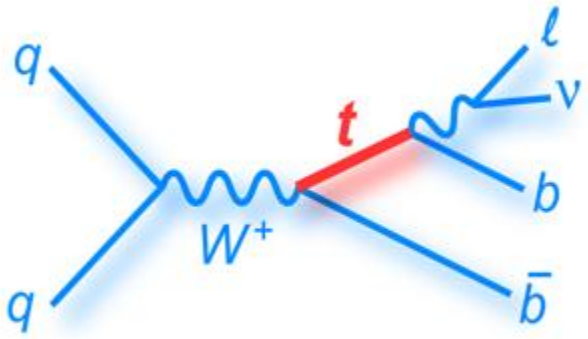

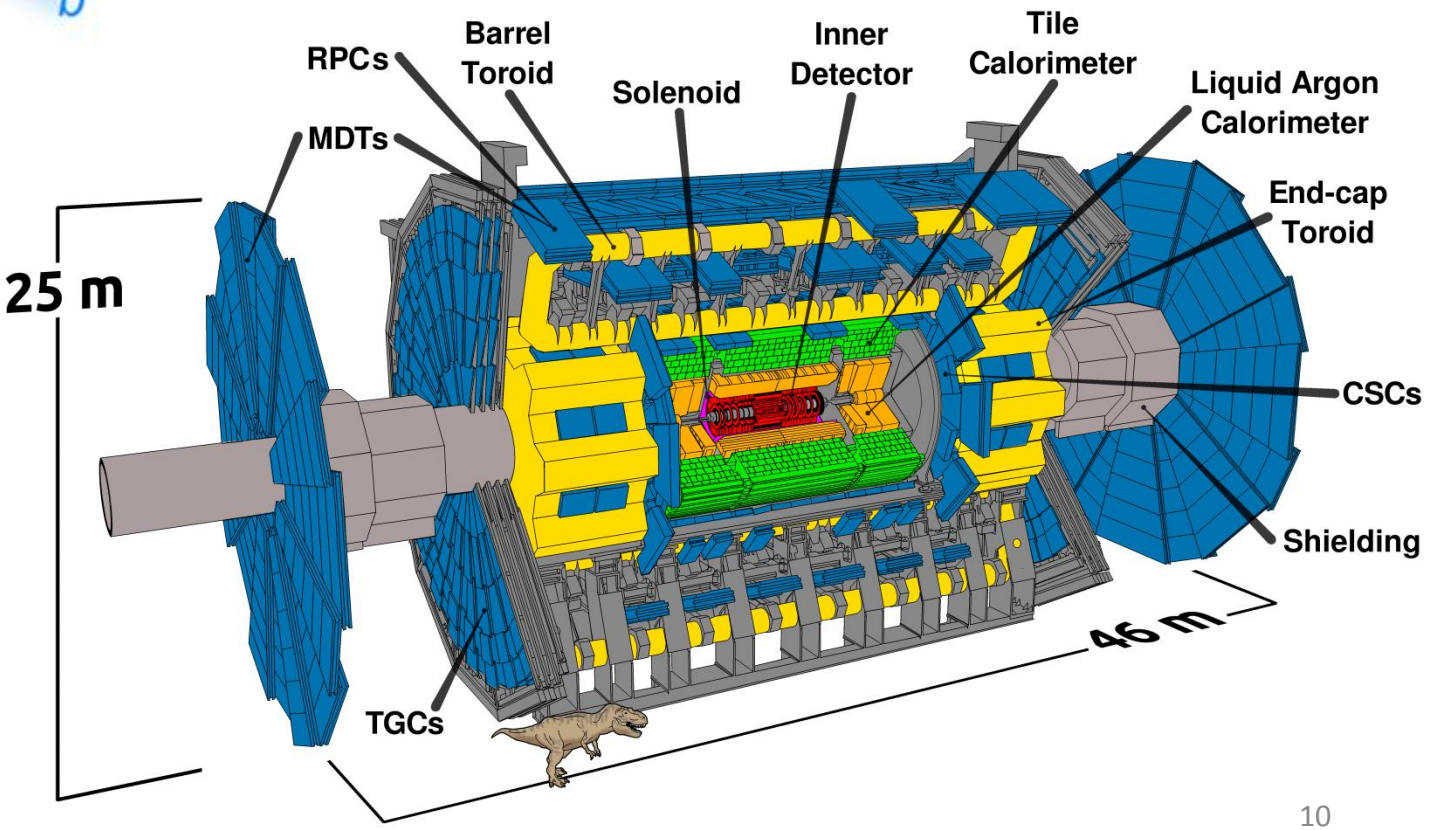

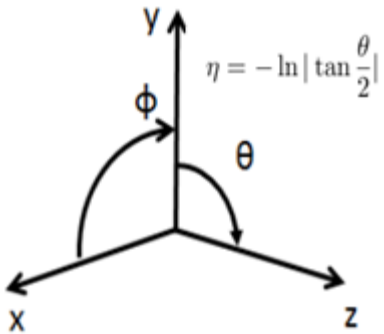

s-channel detection with ATLAS

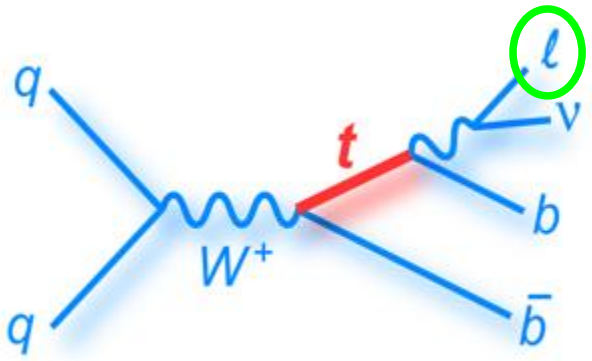

Top pair semileptonic decay, ATLAS EVENT DISPLAY

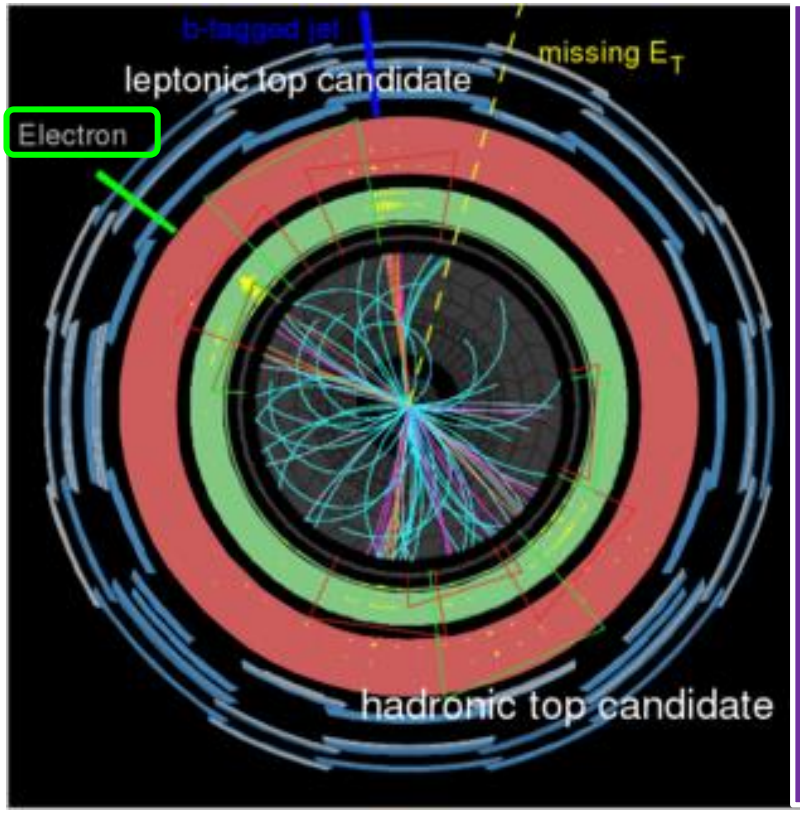

electron

- EM cluster associated to a inner detector track
- Identification: loose/medium/tight quality criteria
- Energy calibration and resolution

- Selection:
  - p_T threshold: 30 GeV
  - inner detector acceptance: $|\eta|<2.47$
  - isolation

s-channel detection with ATLAS

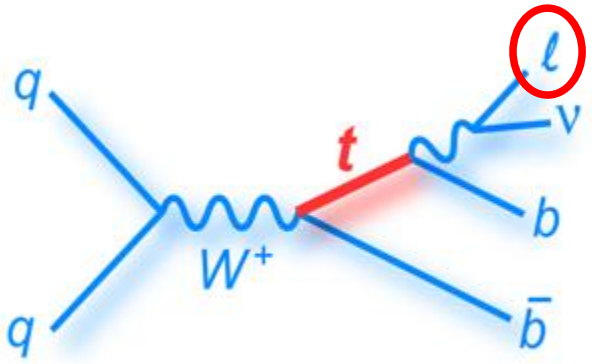

Top pair semileptonic decay, ATLAS EVENT DISPLAY

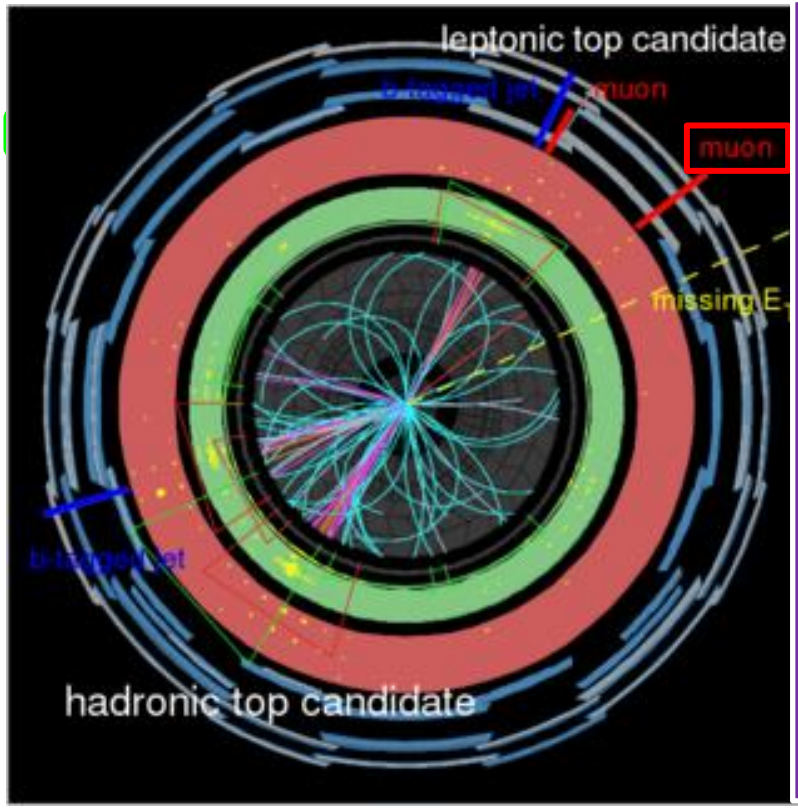

muon

- Independent track reconstruction in
  - muon spectrometer
  - inner detector
- Identification
- Momentum calibration and resolution

- Selection:
  - p_T threshold: 30 GeV
  - $|\eta|<2.5$
  - isolation

s-channel detection with ATLAS

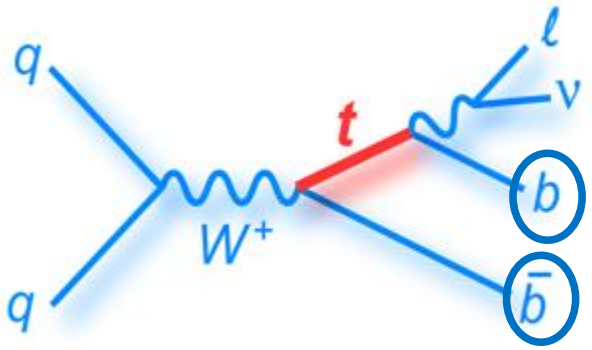

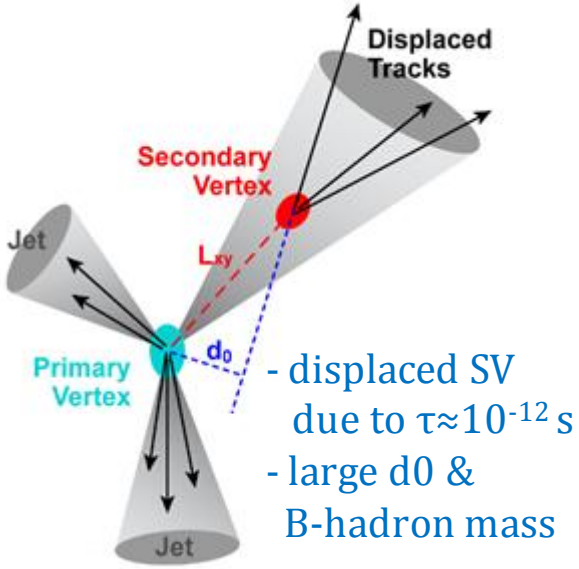

- displaced SV due to $\tau \approx 10^{-12}$ s
- large d0 & B-hadron mass

- semileptonic decay (40%)

Top pair semileptonic decay, ATLAS EVENT DISPLAY

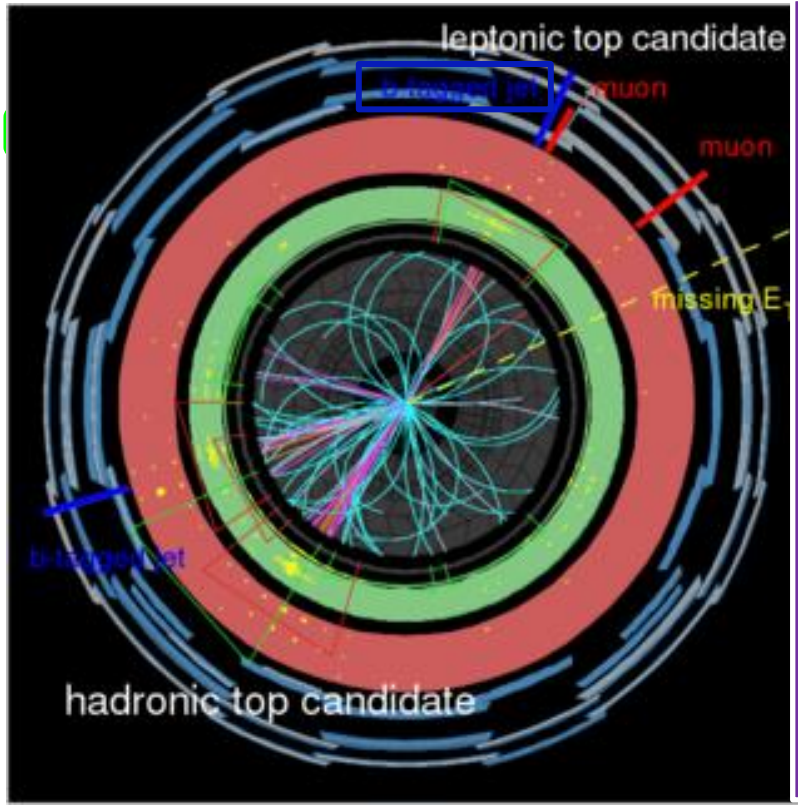

B-jets

- topocluster in hadronic calorimeter
- Identification
- Energy calibration via p_T η-dependent corrections
- b-tagging

- Selection:
  - p_T threshold: 30 GeV
  - inner detector acceptance: $|\eta|<2.5$
  - b-tagging with MV1 algorithm

s-channel detection with ATLAS

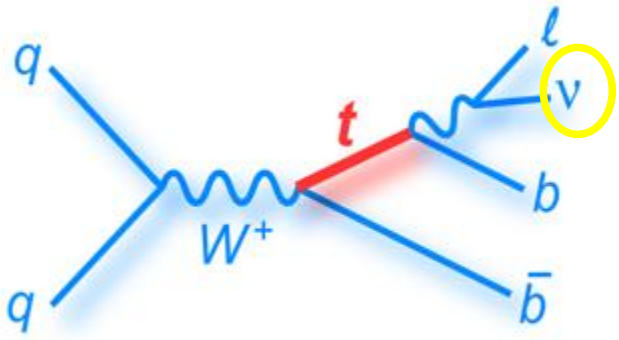

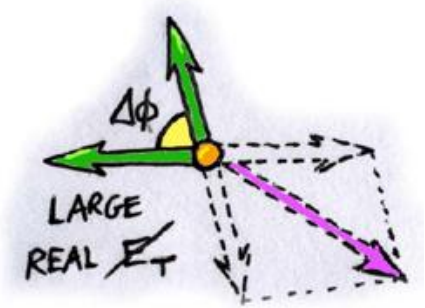

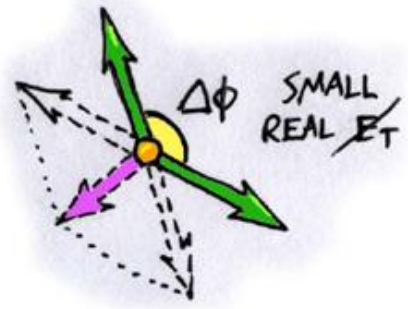

Top pair semileptonic decay, ATLAS EVENT DISPLAY

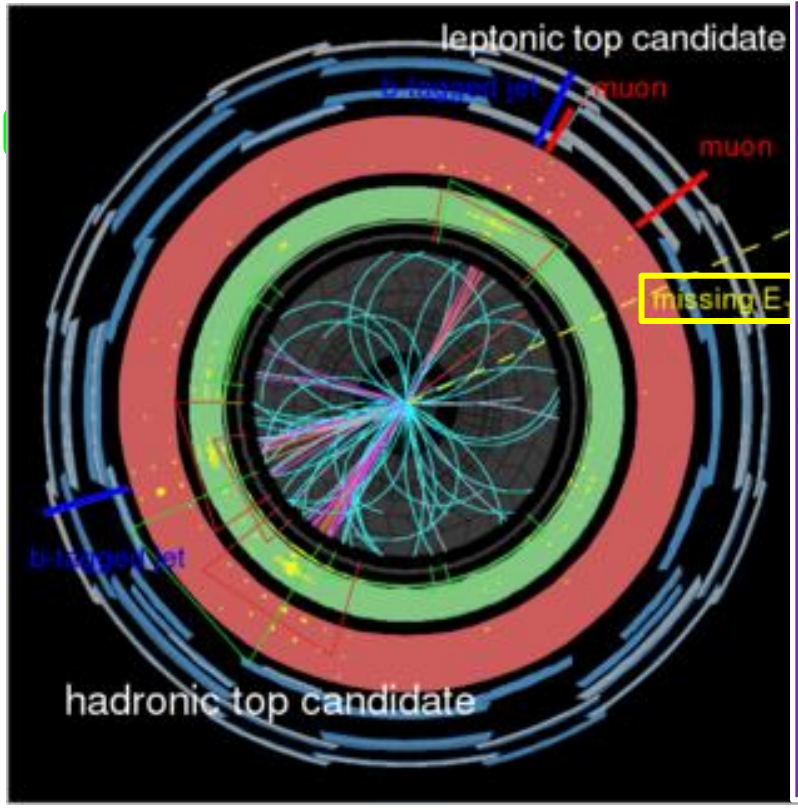

Missing transverse momentum

- Event momentum imbalance in the plane perpendicular to the beam axis
- Energy calibration and resolution

- Selection:
  $E_T^{miss} > 30$ GeV
- Neutrino reconstruction:
  $p_T : E_t^{miss}$, p_z: W-boson pole-mass constraint

Search for s-channel single top quark production in p-p collisions at $\sqrt{s}$=8 TeV with the ATLAS detector

ATLAS Draft

TOPQ-2014-03

Version: 2.0

To be submitted to: Phys. Lett. B.

Analysis Team

B. Alvarez Gonzalez (*), O. M. Kind (*), A. Lleres (*),
C. Monini (*), P. Rieck, S. Stamm

Signal preselection

Data collected in 2012, integrated luminosity: 20.3 fb^{-1}

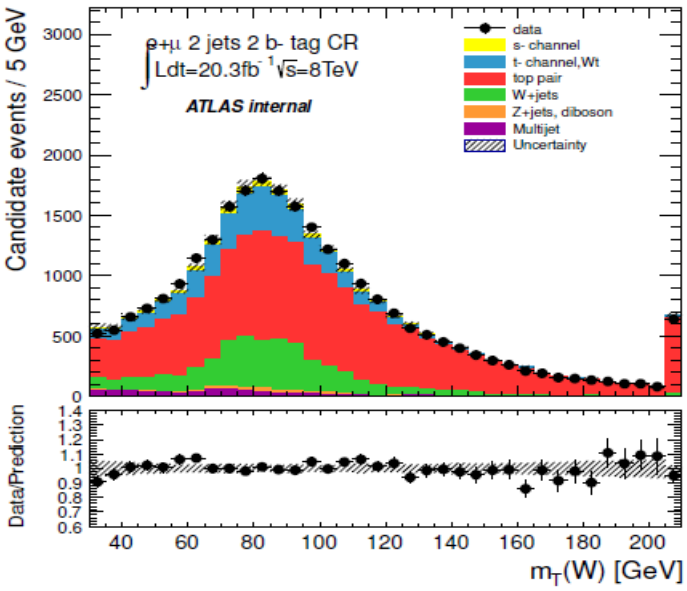

Single lepton event trigger

Preselection:

- 1 isolated electron or muon
- 2 b-tagged jets (MV1 algorithm @70% efficiency)
- missing transverse momentum threshold
- $m_T(W) > 30$ GeV to reduce multijet events

Monte Carlo simulation of physics processes that may fake single top s-channel signature→ interpretation of the ATLAS dataset

Top pairs background

Top pairs production
in the semileptonic and dileptonic decay channels constitutes the main background source
(61% of the total preselected events)

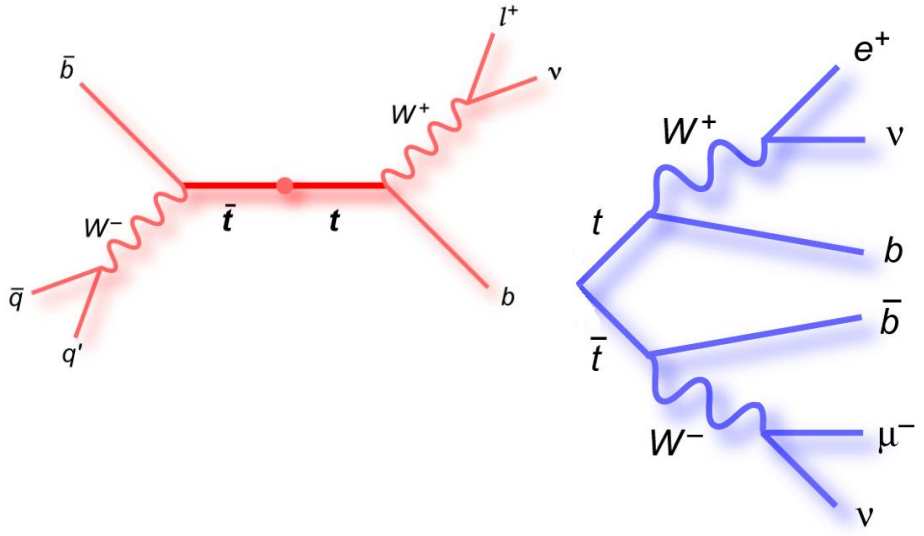

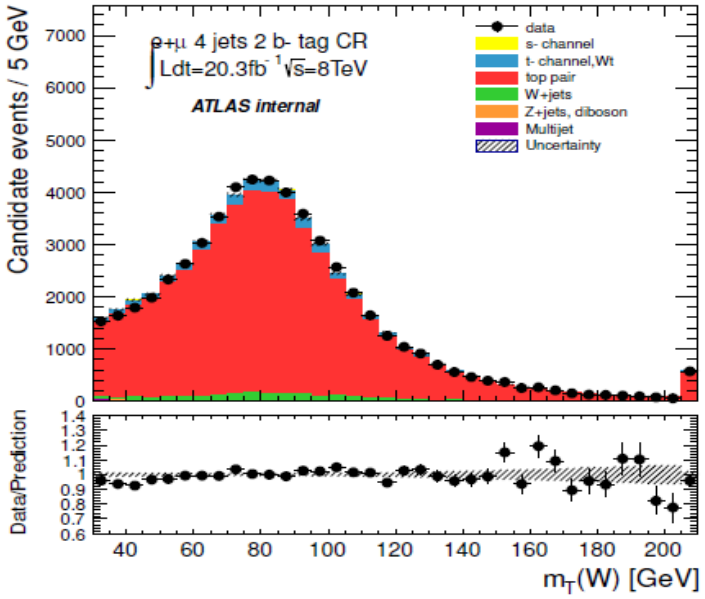

→ analyzed in specific <u>control region:</u>
- same preselection cuts but
- 2 additional jets,
  without b-tagging requirement

Modelled with MC simulation samples

W+jets background

W+ light and heavy jets events

Second background source, representing the 15% of the total preselected events

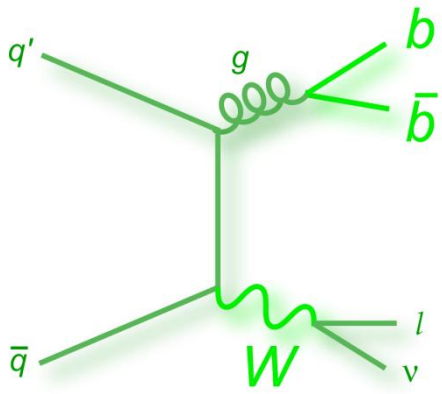

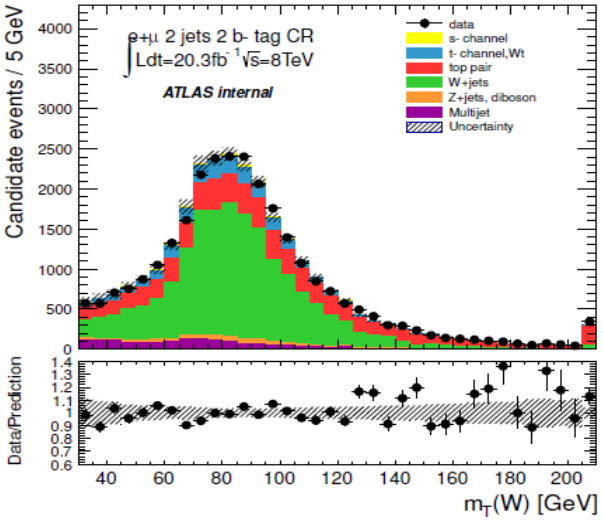

→ analyzed in a specific <u>control region:</u>
- same preselection cuts but
- lower jet p_T threshold
- looser b-tagging criterion
- veto to be orthogonal to signal region

Distributions modelled with MC templates,
theoretical cross sections corrected by a data-driven overall normalization
(likelihood fit of the distribution used to measure the s-channel cross section)

Minor background sources

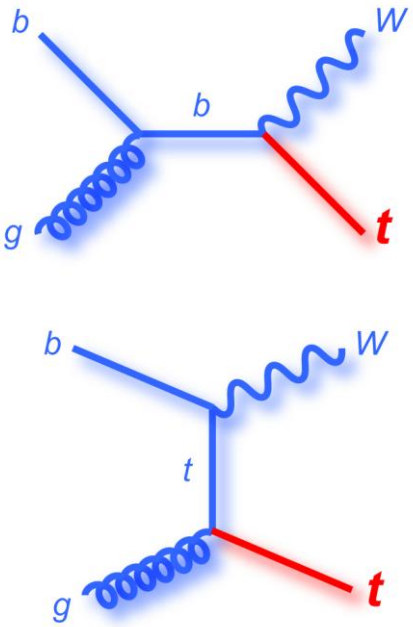

Single top events

Low production rate,
but signatures close to the signal one

t-channel & Wt production merged
to reduce statistical fluctuations

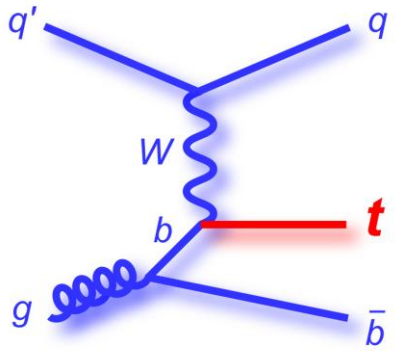

Z+jets and diboson (WW, WZ, ZZ) productions

Negligible contribution, processes merged in the analysis

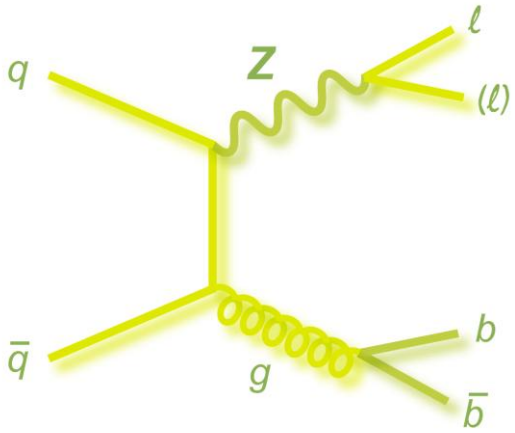

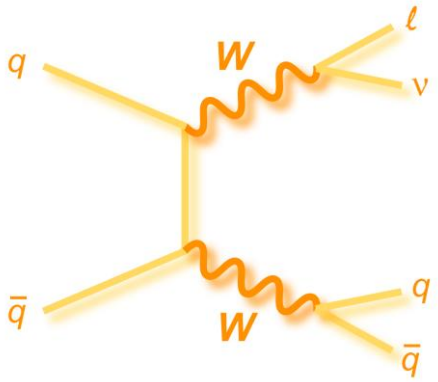

Modelled with
MC simulation samples

Multijet background

Multijet production

Very high rate, shares the signal signature in case of:
- Jets misidentified as leptons (j)
- b-jets or long-lived mesons semileptonic decays… (non-prompt l)

} fake lepton

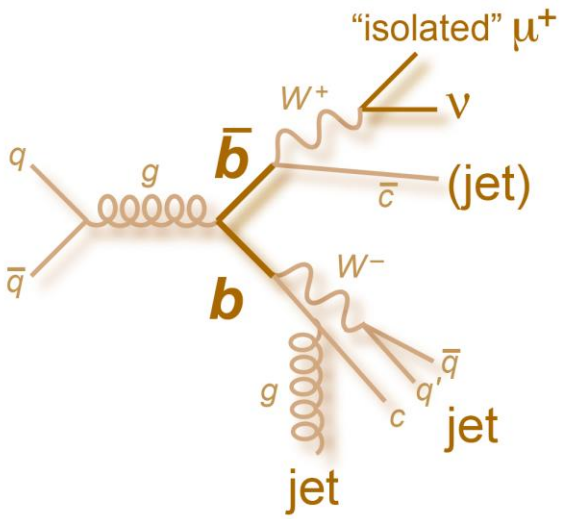

Misreconstruction mechanisms detector-dependent
→ data-driven **matrix method**

- Normalization:

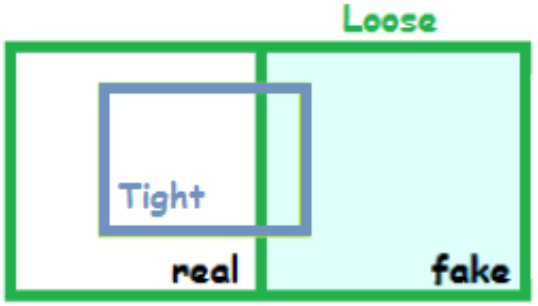

Tight sample:
isolation cut reduces
fake lepton contribution

$$N^{loose} = N^{loose}_{real} + N^{loose}_{fake}$$

$$N^{tight} = \epsilon_{real} N^{loose}_{real} + \epsilon_{fake} N^{loose}_{fake}$$

- Modelling : reweighting of the "loose" data sample

Analysis strategy

After the event preselection:

- signal purity: 2.8%
- considerable overlap in the signal and background distributions

1) further signal selection:

- p_T of the jet used to reconstruct the top > 50 GeV
- $m_T(W)$ > 50 GeV

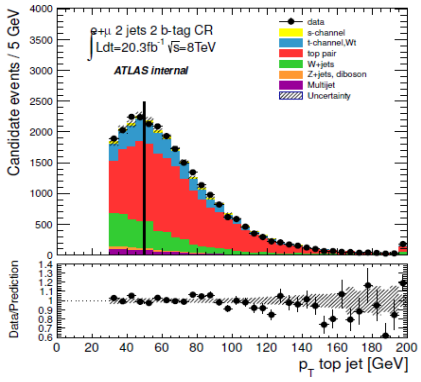

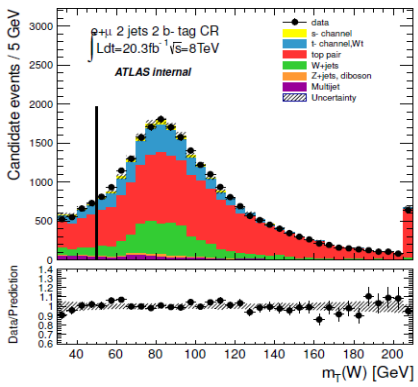

Process	Pre-selection	Selection
s-channel	674±6	457±5
t,Wt-channels	3752±45	2264±34
$t\bar{t}$	15252±67	10206±54
W+light jets	468±66	189±43
W+heavy flavour	3862±72	1985 ±51
Z+jets	293±16	108±7
Multijet	944±472	279±139
Total expectation	24958 ±273	15433±124
Data	25900±161	16031±127
S/B [%]	2.8	3.1

2) discriminant variable for the fit: multivariate techniques
Boosted decision trees (BDT) output distribution

Boosted decision trees

Binary trees made by nodes that split recursively in 2

- Training sample: MC templates for signal and background

- Sequential selection implemented by cutting on the variable that accords the best signal-background separation
  → subdivision of the phase space into orthogonal zones (S or B-like), no event rejection

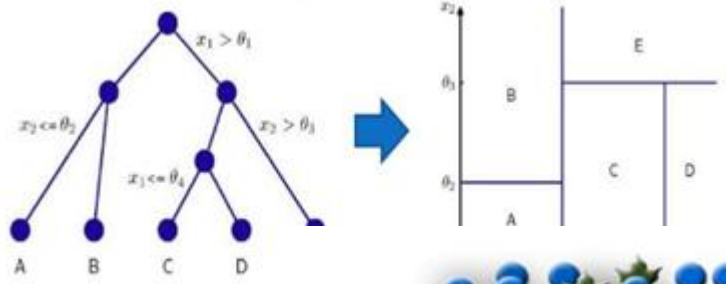

- Instability depending on excessive optimization for the training sample overcame with stopping criteria and boosting (forest of trees)

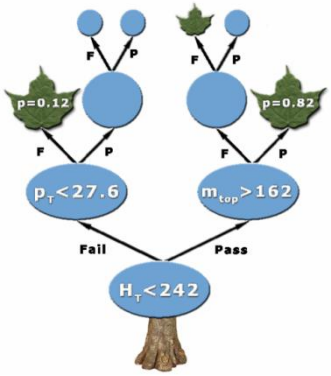

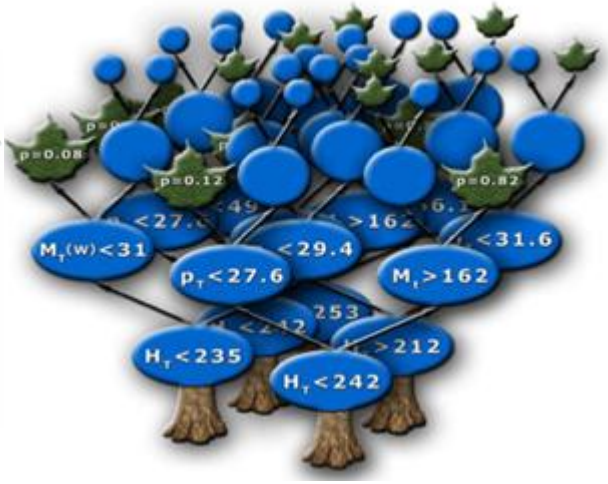

- Machine learning: application of the algorithm on data

BDT inputs

1) Choice of the background sources for the training: ttbar & W+jets preselected events

2) Selection of the kinematic and topological input variables

- good modelling
- high separation power, evaluated via the parametric function $\begin{cases} x = F_s(\epsilon) \\ y = F_b(\epsilon) \end{cases}$

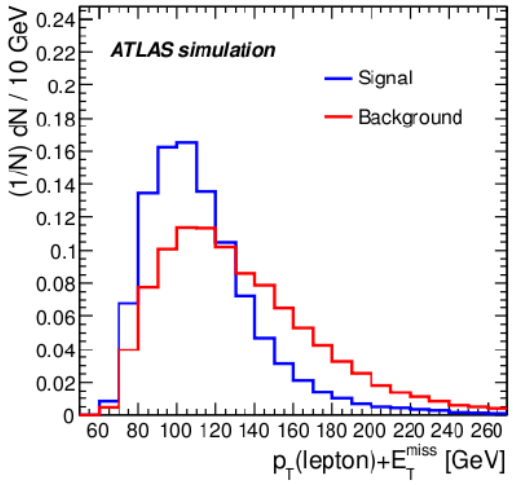

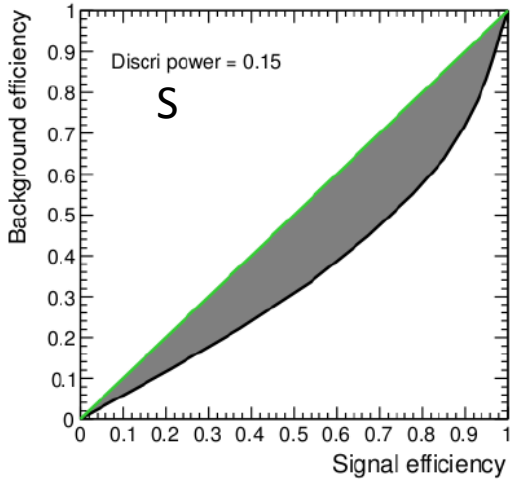

cumulative functions for S & B events

BDT inputs

1) Choice of the background sources for the training: ttbar & W+jets preselected events

2) Selection of the kinematic and topological input variables

Input variable list optimized in order to minimize
the total expected uncertainty on the s-channel cross section: 19 selected

Variable	S	Definition
$\lvert\Delta\phi(t2, j1)\rvert$	0.17	$\lvert\Delta\phi\rvert$ between the leading jet and the top quark ($Top_j2\nu l$ [1])
$\lvert\Delta\phi(t1, j2)\rvert$	0.16	$\lvert\Delta\phi\rvert$ between the subleading jet and the top quark ($Top_j1\nu l$ [1])
$p_T(l) + E_T^{miss}$	0.15	Sum of lepton p_T and missing transverse energy
E_{T}^{miss}	0.11	Missing transverse energy
$m_{\mathrm{T}}(W)$	0.10	Transverse mass of the W-boson
$p_{\mathrm{T}}(l)$	0.09	Transverse momentum of the lepton
$\lvert\Delta\eta(l, j1)\rvert$	0.07	$\lvert\Delta\eta\rvert$ between the lepton and the leading jet
H_{T}	0.07	Scalar sum of jets p_T, lepton p_T and missing transverse energy
$\lvert\Delta\eta(t2, j1)\rvert$	0.07	$\lvert\Delta\eta\rvert$ between the leading jet and the top quark
$\lvert\Delta\phi(j1, j2)\rvert$	0.07	$\lvert\Delta\phi\rvert$ between the jets
$\lvert\Delta\phi(l, E_{\mathrm{T}}^{miss})\rvert$	0.06	$\lvert\Delta\phi\rvert$ between the lepton and the missing transverse energy
$\lvert\Delta\eta(l, j2)\rvert$	0.05	$\lvert\Delta\eta\rvert$ between the lepton and the subleading jet
$\lvert\Delta\eta(\nu, j_{no\ top})\rvert$	0.05	$\lvert\Delta\eta\rvert$ between the neutrino and the jet not used to reconstruct the top
$p_{\mathrm{T}}(j1, j2)$	0.05	p_T of the system composed by the two jets
$W\ helicity$	0.05	W helicity from the top quark (reconstructed via the leading jet) decay[2]
$\cos\theta(E_{\mathrm{T}}^{miss}, j2)$	0.05	Cosine of the angle between E_T^{miss} and the subleading jet
$m(l, j2)$	0.05	Mass of the system composed by the lepton and the subleading jet
$\cos\theta(Top_j2\nu l)$	0.05	Top (reconstructed via the subleading jet) spin correlation in helicity basis[3]
$\cos\theta(Top_j1\nu l)$	0.05	Top (reconstructed via the leading jet) spin correlation in helicity basis[3]

BDT inputs

1) Choice of the background sources for the training: ttbar & W+jets preselected events

2) Selection of the kinematic and topological input variables

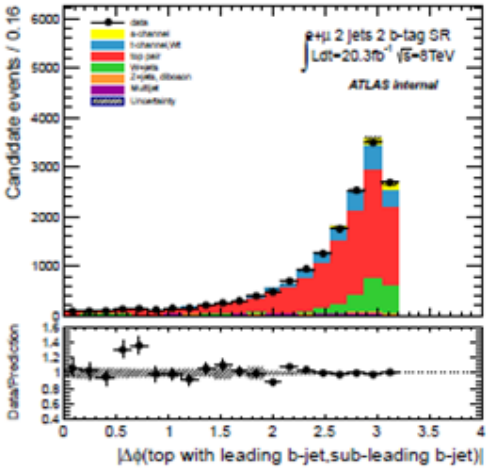

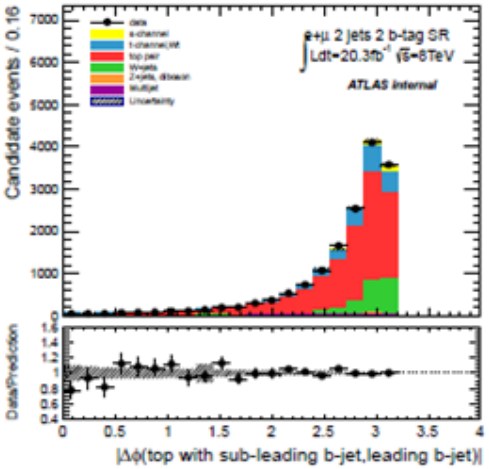

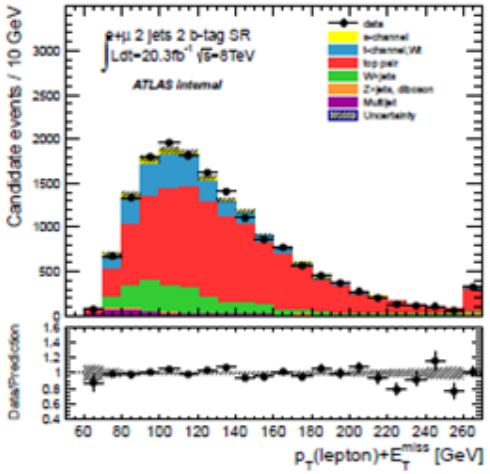

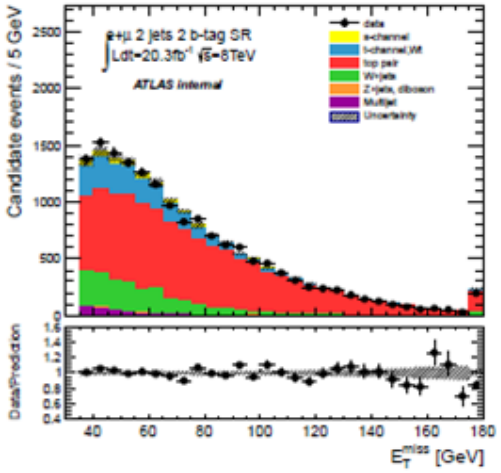

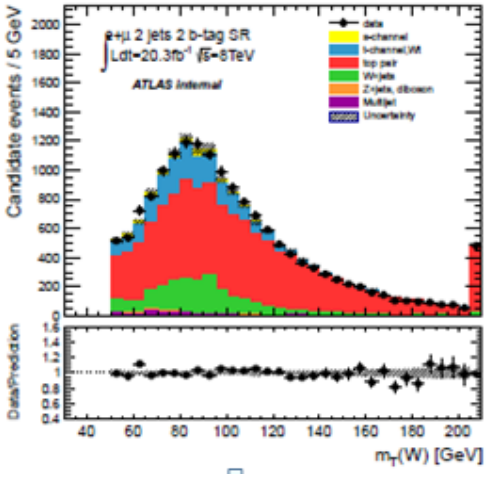

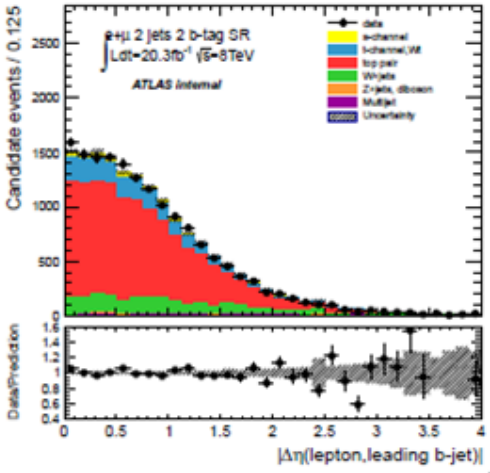

BDT application

1) Choice of the main background sources for the training

2) Selection of the kinematic and topological input variables

3) Optimization of the BDT configuration

- to maximizing the BDT separation power
- and avoid overtraining

Parameter	Type/Value
Boosting algorithm	Gradient boosting
nTrees	350
MaxDepth	3
MinNodeSize	18

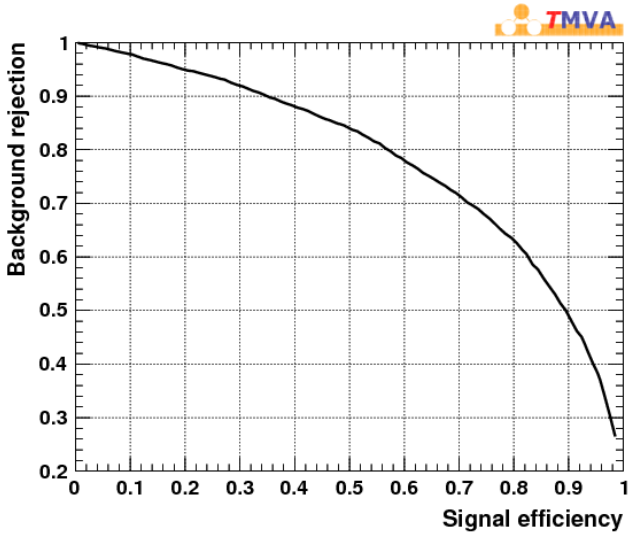

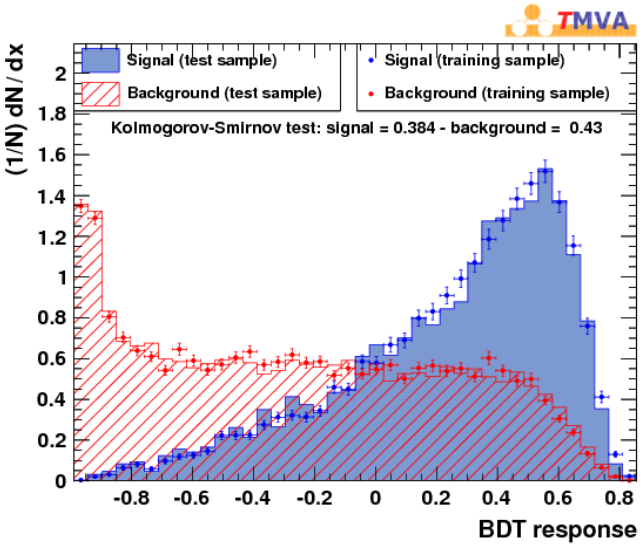

BDT application

1) Choice of the main background sources for the training

2) Selection of the kinematic and topological input variables

3) Optimization of the BDT configuration

4) Application of the BDT algorithm to data → fit of the output distribution

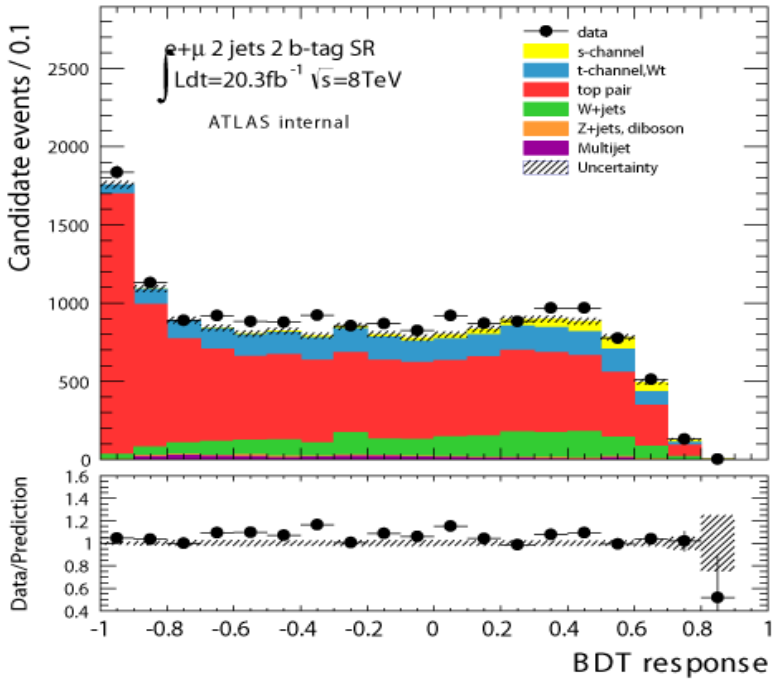

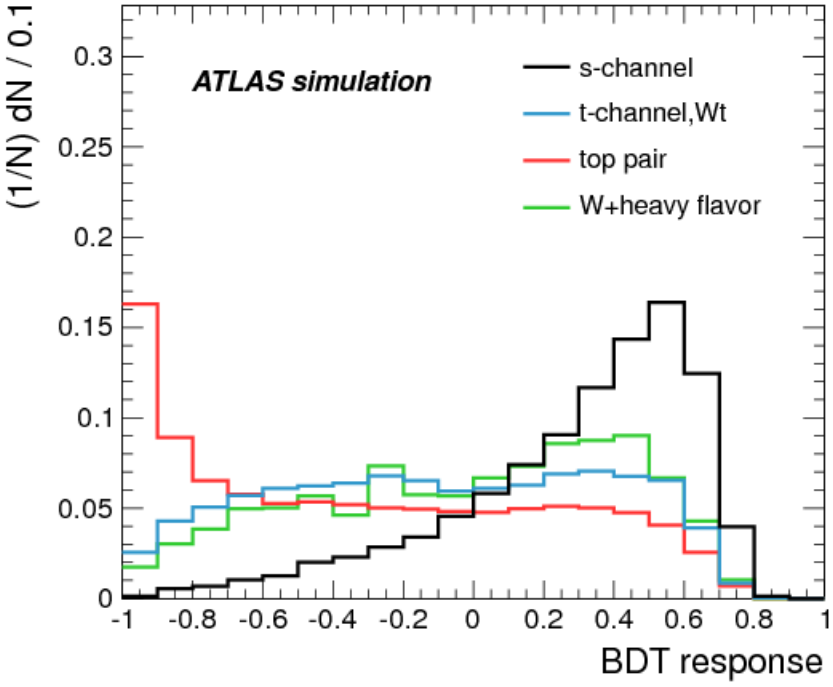

Maximum likelihood fit

Maximum likelihood fit to the data of the BDT classifier

$$L(\beta^s;\beta_j^b) = \prod_{k=1}^{Nbins} \frac{e^{-\mu_k}\mu_k^{n_k}}{n_k!} \prod_{j=1}^{Nbackgrounds} G(\beta_j^b;1.0,\Delta_j)$$

n. of observed events

expectation value

relative uncertainty of the bkg

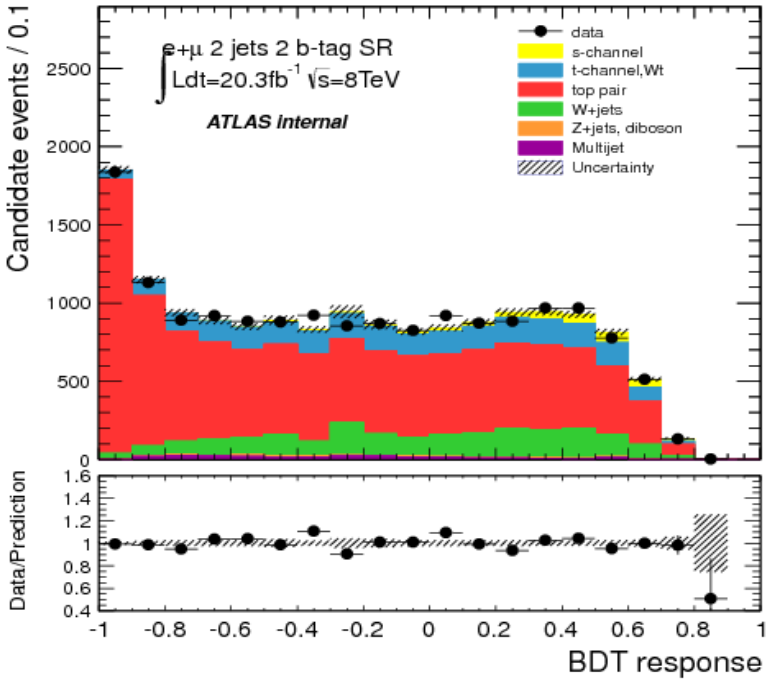

Extraction of the nominal signal cross section: $\beta_s \cdot \sigma_s$

Process	β
s-channel	0.89±0.32
$t\bar{t}$	1.05±0.02
t-channel, Wt	1.02±0.05
W+jets	1.12±0.15
Z+jets, diboson	1.07±0.59
Multijet	1.00 (fixed)

Sources of uncertainties

- Data and simulation statistics
- Experimental uncertainties:
  - luminosity
  - energy scale & resolution of the reconstructed objects
  - lepton trigger, identification, reconstruction efficiency
  - jet reconstruction and tagging efficiency
- Theoretical and data-driven normalizations of the physics processes
- Modelling:
  - ISR/FSR
  - signal generator scale
  - MC generator and parton shower
  - PDFs

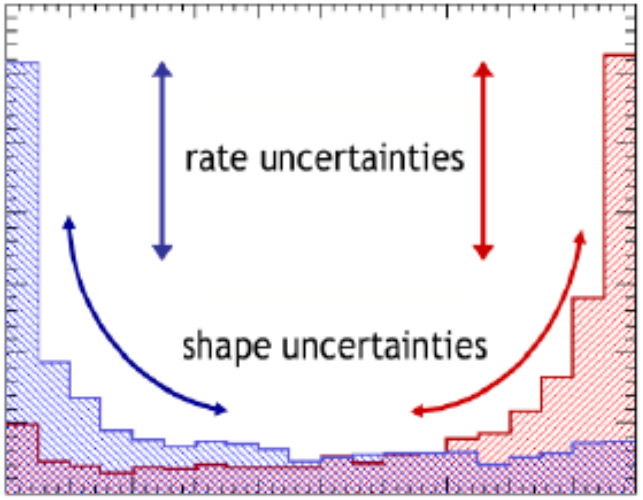

are integrated via pseudo-experiments including:

- rate variations:

$$\nu_j^{gen} = \widetilde{\nu}_j \cdot \beta_j^{gen} \cdot \left\{ 1 + \sum_{i=1}^{S} |\delta_i| \cdot (H(\delta_i) \cdot \epsilon_{i,j+} + H(-\delta_i) \cdot \epsilon_{i,j-}) \right\}$$

- shape variations:

$$\alpha_{jk}^{gen} = \left[\alpha_{jk} + \sum_i |\delta_i| \cdot \left(H(\delta_i) \cdot \Delta\alpha_{ijk}^{+} + H(-\delta_i) \cdot \Delta\alpha_{ijk}^{-} \right) \right]$$

Cross section extraction

→**Total uncertainty**: modified standard deviation to account for asymmetries

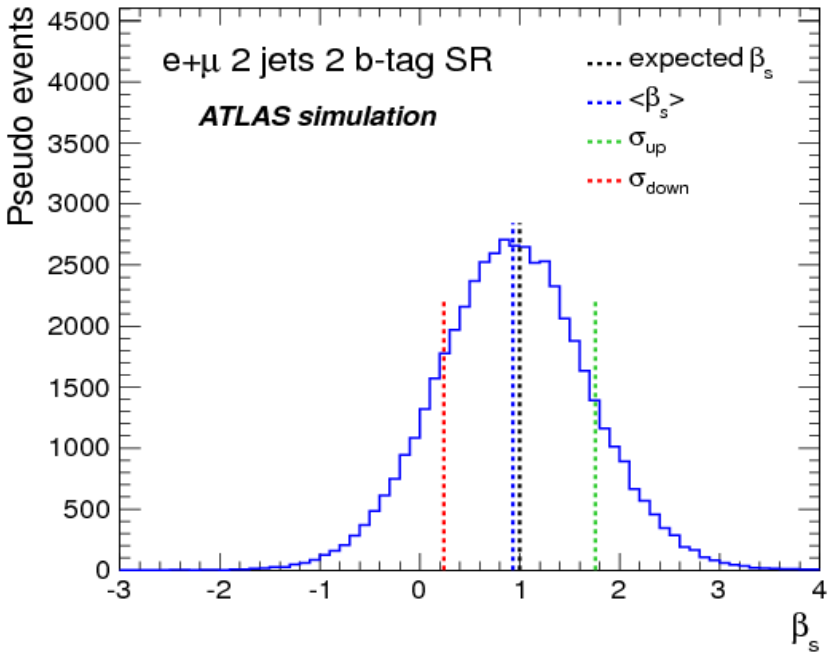

In agreement with the SM prediction:

$$\sigma_s = 5.0 \pm 1.7(stat) \pm 4.0(syst) \text{ pb} = 5.0 \pm 4.3 \text{ pb}$$

$$\sigma s, SM = 5.61 \pm 0.21 \; pb$$

→ **Individual contributions:**

Source	$\Delta\sigma/\sigma$ [%]
Data statistics	±35
Simulation statistics	±29
$E_{\mathrm{T}}^{\mathrm{miss}}$ scale	±54
$E_{\mathrm{T}}^{\mathrm{miss}}$ resolution	+0/-3
Jet energy scale	±39
Jet energy resolution	±5
Jet tagging efficiencies	±4
Jet reconstruction efficiency	< 1
Lepton energy scale/resolution	< 1
Lepton efficiencies	+2/-1
Signal modelling & scale	±11
$t\bar{t}$ modelling	±6
W+jets shape modelling	±8
ISR/FSR	±3
PDF	< 1
Background normalization	±7
Multijet normalization	±12
Integrated luminosity	±2
Total systematic	±80
Total	±87

Significance & limit

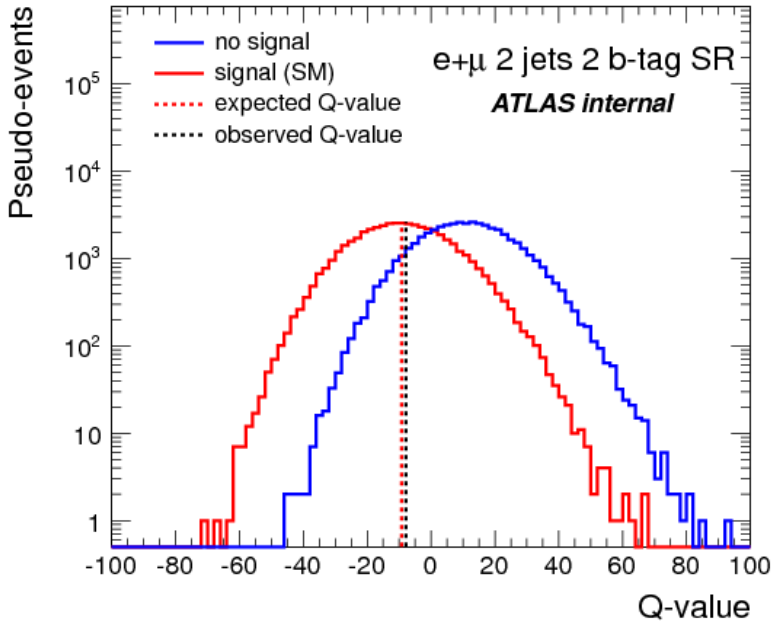

Sensitivity of the measurement:
1.3 (1.4 exp) standard deviation

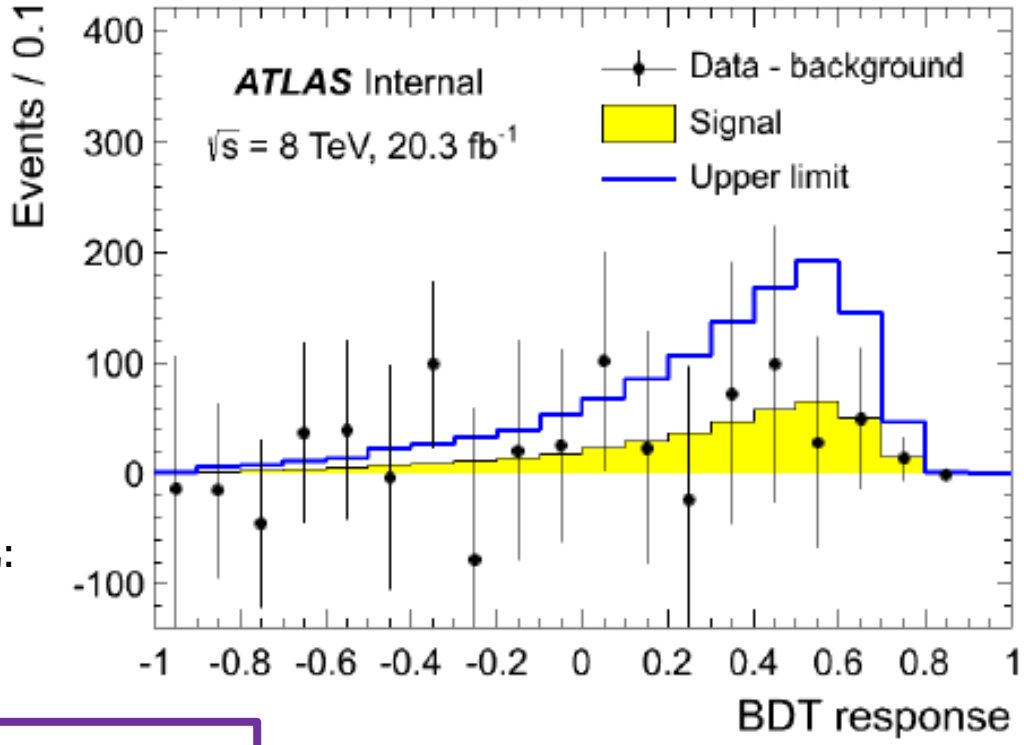

Extraction of a CLs limit at 95% CL:

$CLs = p_{s+b}/(1-p_b) < 5\%$

$$\sigma_s < 14.6\ (7.9\ \text{exp})\ \text{pb} = 2.6\ \ (1.4\ \text{exp})\,\sigma_{s,SM}$$

Conclusion

Finalization of two searches for the electroweak production of top quark in the s-channel with the full ATLAS dataset collected at 7 and 8 TeV.
Similar multivariate analyses, boosted decision trees discriminants.

- **7 TeV**: CLs exclusion limit at 95%: CL σ_s <21.7 pb
  → improved the previous ATLAS result (L=0.70 fb^{-1}, cut-based selection)

- **8 TeV**: cross section measurement (after TeVatron's discovery): $\sigma_s = 5.0 \pm 4.3$ pb
  corresponding to 1.3 standard deviations,
  in agreement with CMS recent result: $\sigma_s = 6.2\ ^{+8.0}_{-5.1}$ pb

Perspectives

- Implement matrix element to improve signal discrimination

- Reduce the impact of statistical and systematic uncertainties

- Analysis will not be eased at higher center of mass energies
  since σ_s increases with $\sqrt{s}$ less steeply than the main backgrounds cross sections

MERCI
pour votre attention

Backup

Single top cross sections

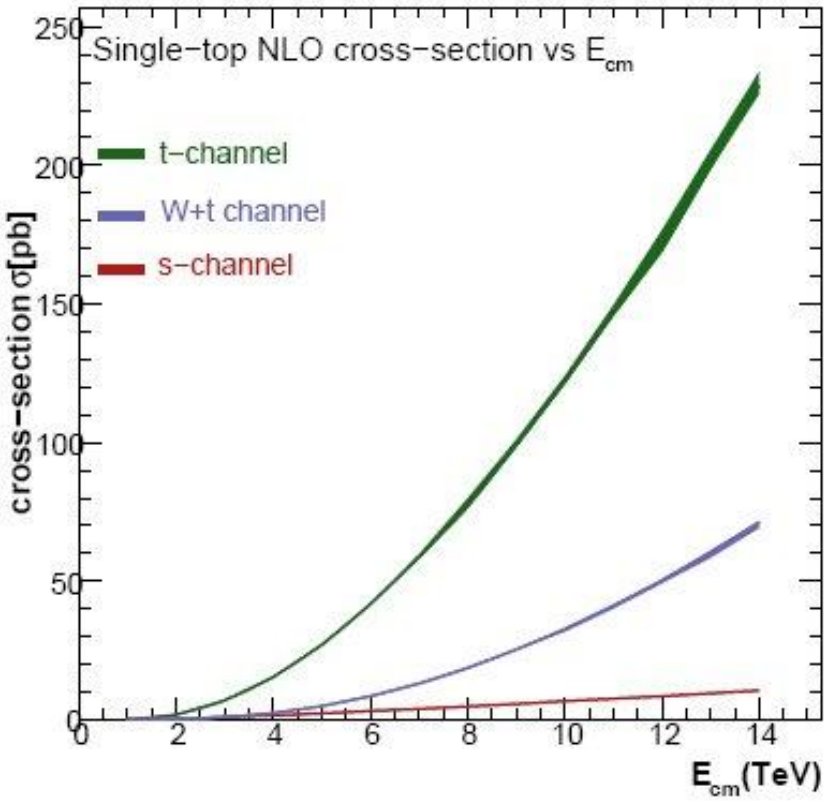

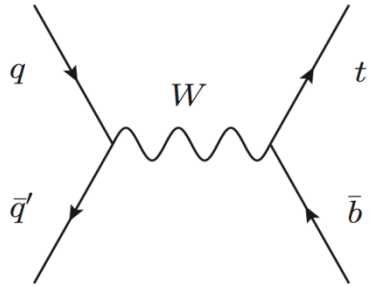

s- channel

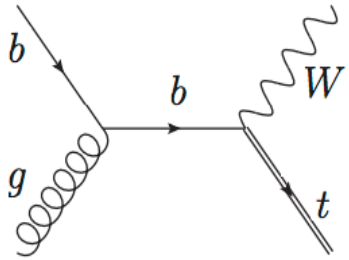

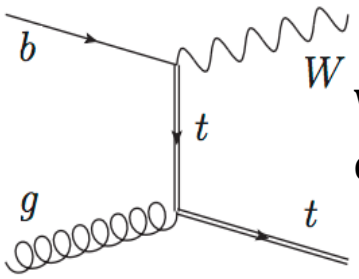

Wt- channel

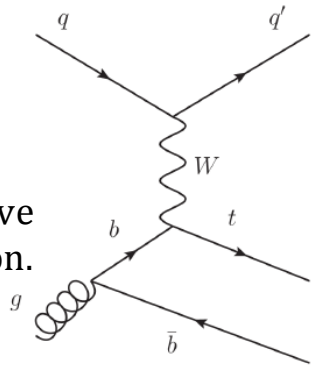

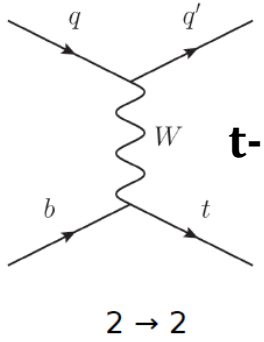

t- channel

b-quark splitted from a gluon brings a non perturbative contribution when the b-quark is collinear to the gluon.

In this case, the perturbative calculation can be restored by the 2→ 2 diagram with a PDF for the b-quark in the initial state instead of a gluon splitting

V_{tb} calculations

- **Direct measurements**: single top
- **CKM unitarity**: top pair decays $R = \frac{\mathcal{B}t \to Wb}{\mathcal{B}t \to Wq} = \frac{|V_{tb}|^2}{\sum_{q=1}^{3} |V_{tq}|^2} = |V_{tb}|^2$
- **Indirect measurements**:
  - leading contribution to mixing amplitude of $B_{d/s}^0$ $B_{d/s}^0$ from electroweak box diagram, $(V_{td}^* V_{tb})^2$

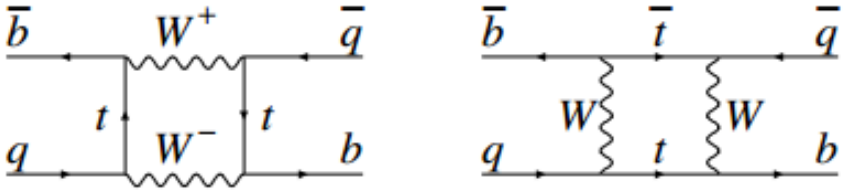

Figure 1: Dominant box diagrams for the $B_q^0 \to \overline{B}_q^0$ transitions ($q = d$ or s). Similar diagrams exist where one or both t quarks are replaced with c or u quarks.

- radiative decay $b \to \gamma s$

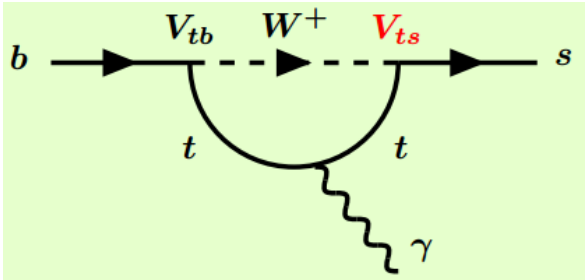

Model independent Vtb

• **Model independent constraints on the CKM matrix** (which rotates the electroweak interaction eigenstates into the mass eigenstates $Q'_L = V_{CKM}\ Q_L$)

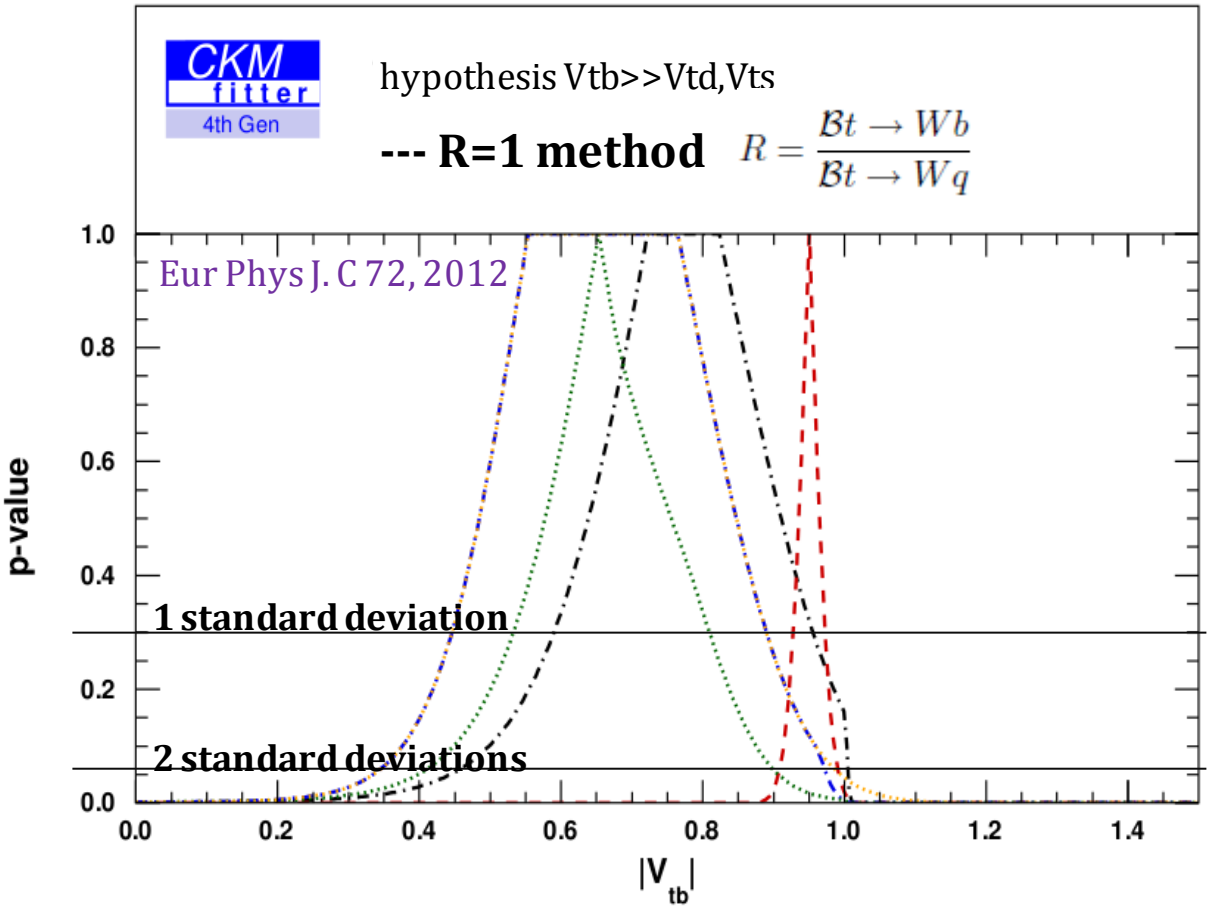

--- 3SM method
3 fermions families,
measured R value (0.90 ±0.04)

--- 4SM method
4 fermions families
$|Vtb|^2+|Vtd|^2+|Vts|^2=1$

--- 4SMTL method
4 fermions families
$|Vtb|^2+|Vtd|^2+|Vts|^2\leq 1$

--- free CKM method
No hypotheses on
top quark couplings

Extra gauge bosons (I)

- **Single top sensitivity to Beyond Standard Model (BSM) physics**

EXTRA GAUGE BOSONS

Top flavor model
Left-right symmetric models
Extradimension theories
…

⇨ postulate a gauge group larger than $SU(3)_C \times SU(2)_L \times U(1)_Y$ and thus further ew mediators W' , Z'

▪ s-channel

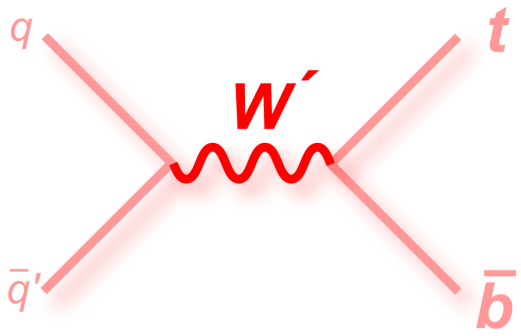

- constructive or destructive interference with the SM W exchange diagrams

- W' produced on shell

▪ t-channel & Wt associate production — negligible effect

Extra gauge bosons (II)

The electroweak part of the SM gauge group is replaced with $SU(2)_1 \times SU(2)_2 \times U(1)_X$ in G(221) models

Couplings with left-handed fermions

Couplings with right-handed fermions

Cat.	Model	$SU(2)_1$	$SU(2)_2$	$U(1)_X$
left-handed	un-unified (UU)	$\begin{pmatrix} u_L \\ d_L \end{pmatrix}$	$\begin{pmatrix} \nu_L \\ e_L \end{pmatrix}$	$Y_{\rm SM}$ for all fermions.
left-handed	non-universal (NU) Top-flavor	$\begin{pmatrix} u_L \\ d_L \end{pmatrix}_{1^{\rm st},2^{\rm nd}}, \begin{pmatrix} \nu_L \\ e_L \end{pmatrix}_{1^{\rm st},2^{\rm nd}}$	$\begin{pmatrix} u_L \\ d_L \end{pmatrix}_{3^{\rm rd}}, \begin{pmatrix} \nu_L \\ e_L \end{pmatrix}_{3^{\rm rd}}$	$Y_{\rm SM}$ for all fermions.
right-handed	left-right (LR)	$\begin{pmatrix} u_L \\ d_L \end{pmatrix}, \begin{pmatrix} \nu_L \\ e_L \end{pmatrix}$	$\begin{pmatrix} u_R \\ d_R \end{pmatrix}, \begin{pmatrix} \nu_R \\ e_R \end{pmatrix}$	$\frac{1}{6}$ for quarks, $-\frac{1}{2}$ for leptons.
right-handed	leptophobic (LP)	$\begin{pmatrix} u_L \\ d_L \end{pmatrix}, \begin{pmatrix} \nu_L \\ e_L \end{pmatrix}$	$\begin{pmatrix} u_R \\ d_R \end{pmatrix}$	$\frac{1}{6}$ for quarks, $Y_{\rm SM}$ for leptons.
right-handed	hadrophobic (HP)	$\begin{pmatrix} u_L \\ d_L \end{pmatrix}, \begin{pmatrix} \nu_L \\ e_L \end{pmatrix}$	$\begin{pmatrix} \nu_R \\ e_R \end{pmatrix}$	$Y_{\rm SM}$ for quarks, $-\frac{1}{2}$ for leptons.
right-handed	fermiophobic (HP)	$\begin{pmatrix} u_L \\ d_L \end{pmatrix}, \begin{pmatrix} \nu_L \\ e_L \end{pmatrix}$		$Y_{\rm SM}$ for all fermions.

1° stage symmetry breaking can proceed via a scalar doublet (D) or triplet (T)

Extra gauge bosons (III)

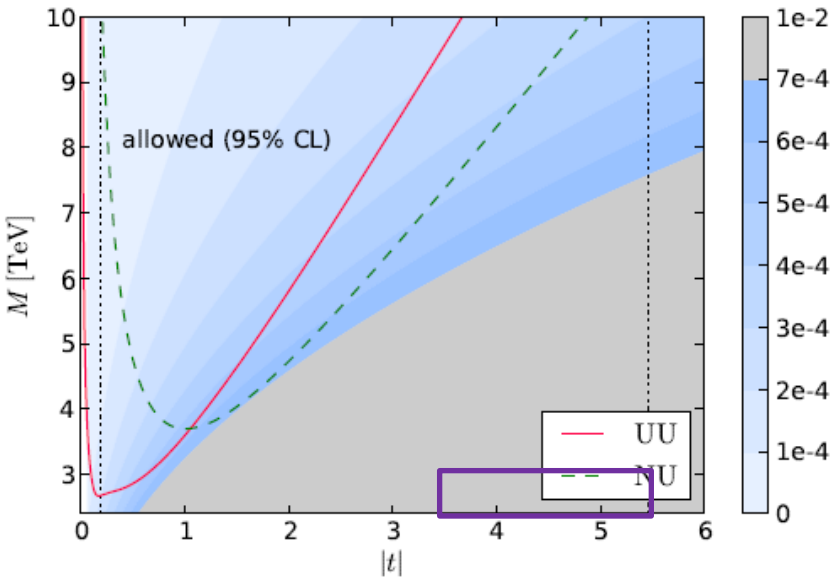

Exclusion limits for *left-handed* models.

$$\mathrm{t} = \mathrm{t}_\theta = \frac{g_W}{g_Y}\ ,\ g_W = \left(\frac{1}{g_1^2} + \frac{1}{g_2^2}\right)^{-1/2},\quad g_Y = g_X$$

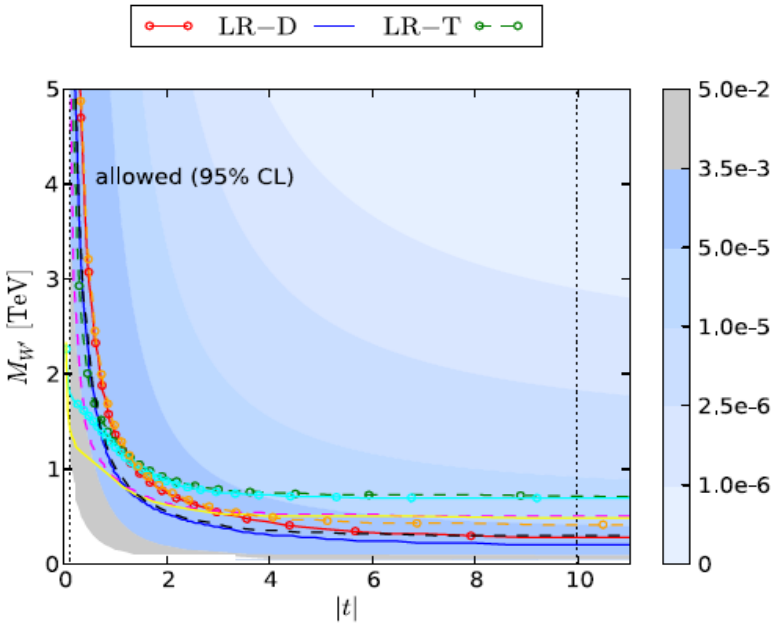

Exclusion limits for *right-handed* models.

$$\mathrm{t} = \mathrm{t}_\phi = \frac{g_X}{g_2},$$

Phenomenological studies

Ph.D. Thesis Tomas Jezo, 2013

$m(W'_R)>1.84$ TeV, $m(W'_L)>1.74$ TeV@ 95% CL

Model independent experimental result

ATLAS-CONF-2013-050

Extra scalar bosons (I)

- **Single top sensitivity to Beyond Standard Model (BSM) physics**

EXTRA SCALAR BOSONS

MSSM… ⇨ (h^0,H^0) CP-even, (A^0) CP-odd, (H^+,H^-)

- s-channel if m($H^{\pm}$)>m(t)

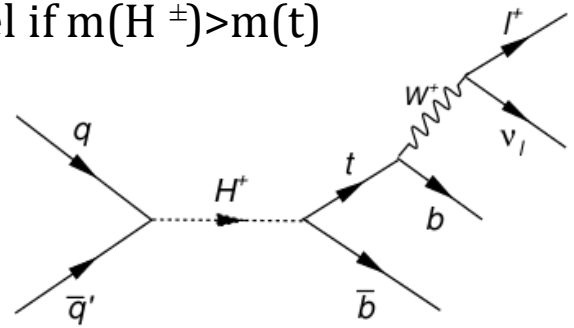

charged Higgs may be produced as a resonance

- all single top channels if m($H^{\pm}$)<m(t)

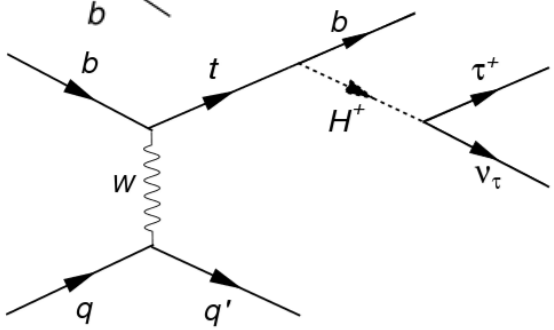

decay could be spotted via an excess in tauonic final states (dominant mode for tanβ>2)

Extra scalar bosons (II)

m(H $^{\pm}$)>m(t) CASE

Recent limits from LHC H/A→ττ: high tanβ excluded for 200< m($H^{\pm}$)<400 GeV
→ relevant tanβ for the analysis not favoured, need confirmation from direct search

JHEP 11 005, 2013 Phenomenological study of the s-channel as source of heavy $H^{\pm}$
simulation LHC events at 14 TeV, mass window cut on charged Higgs

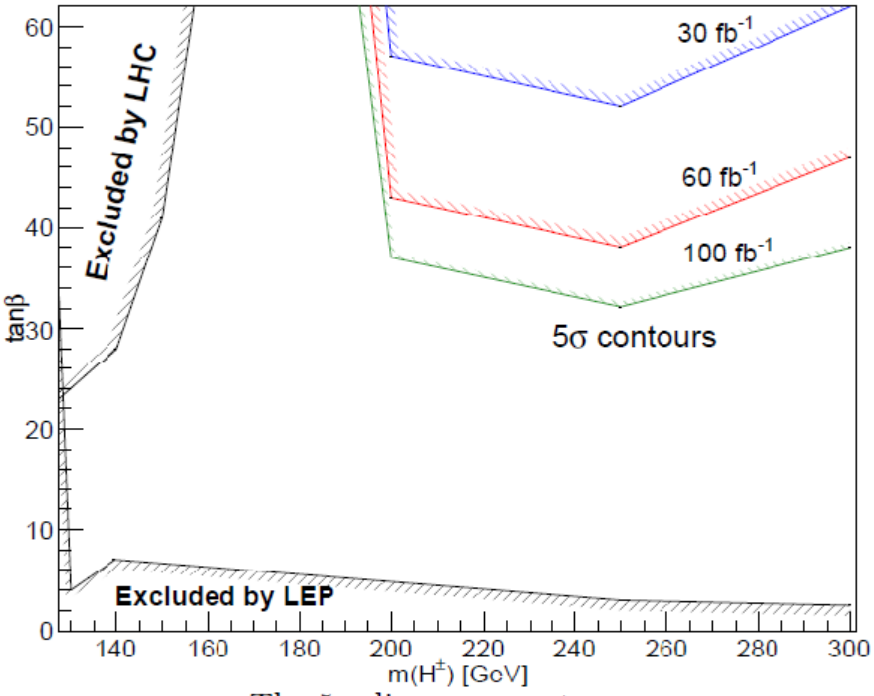

The 5σ discovery contour

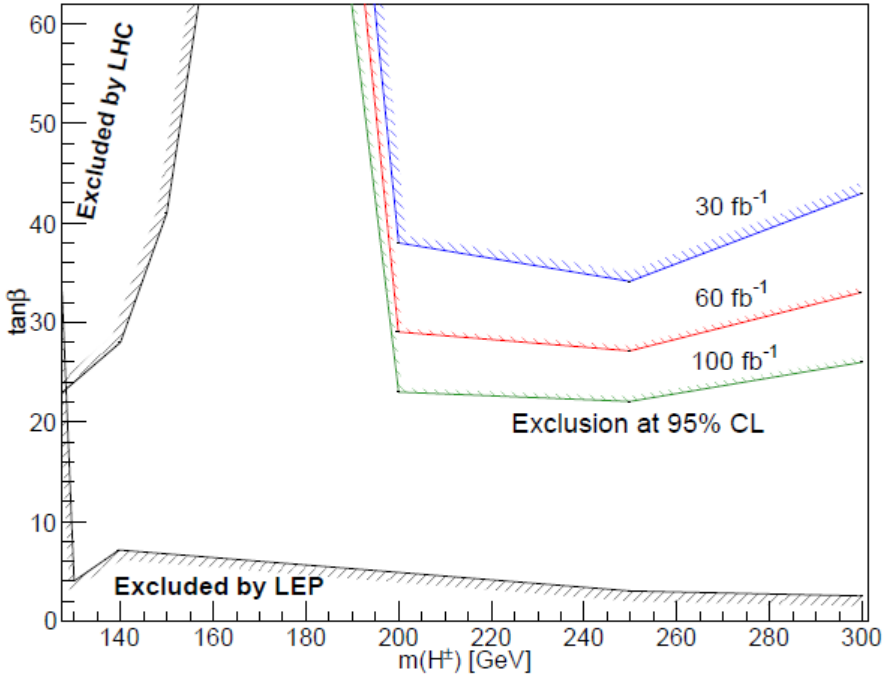

The 95% C.L. exclusion contour.

Extra scalar bosons (III)

m(H $^{\pm}$)<m(t) CASE

JHEP 05 112, 2013 Phenomenological search for light $H^{\pm}$ decay in the t-channel single top
$m(H^{\pm})>125$ GeV due to recent LHC exclusion results ($\tan\beta>10/20$)

simulation LHC events at 14 TeV

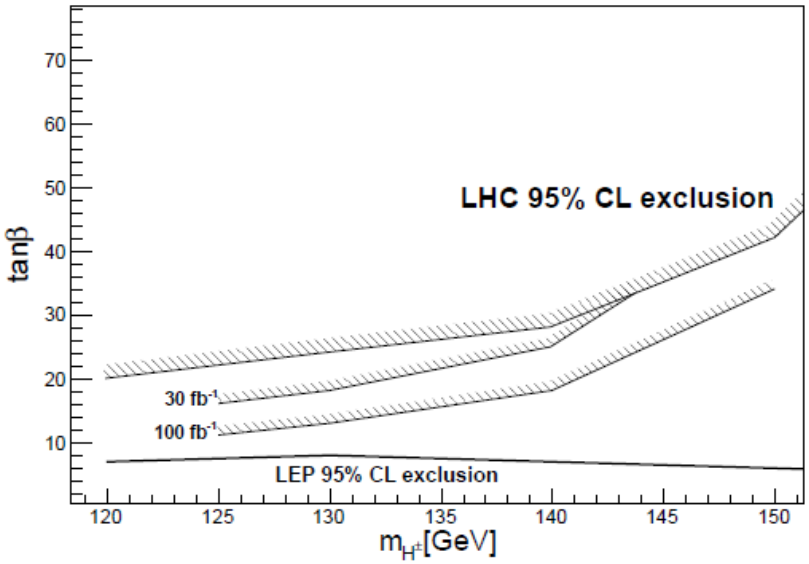

The 5σ contour for different integrated luminosities.

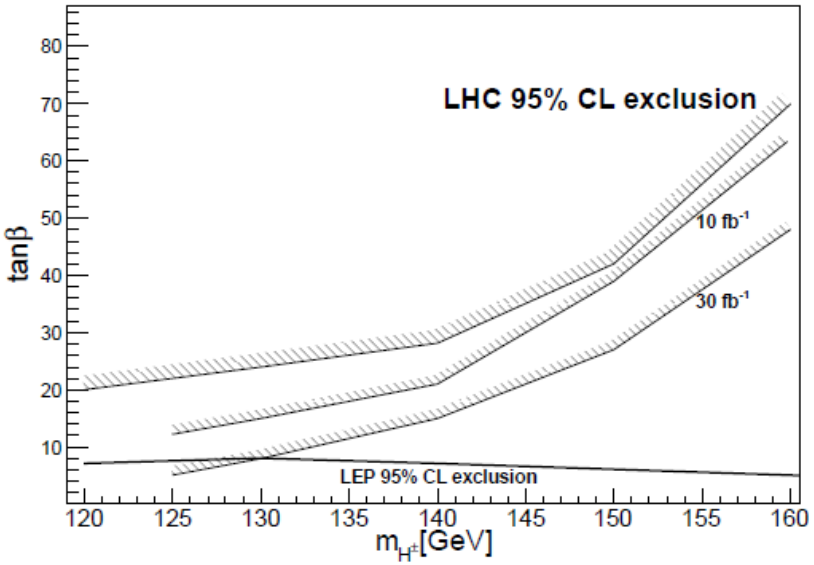

Excluded area at 95% C.L. for different integrated luminosities.

Extra scalar bosons (III)

TECHNIPIONS

- New strong interaction: the technicolor
- Additional massless techni-fermions sensitive to it (left-handed: SU(2)L doublets, Right-handed: SU(2)_L singlets)
- Global chiral symmetry of the fermions spontaneosuly broken by the formation of techni-fermion condensates (technipions) which acquire mass together with Z&W

In order to provide fermion masses and mixing angles an extended technicolor gauge interaction involving both ordinary and techni-fermions was proposed.

In the top color assisted technicolor the top quark participates in this new strong interaction which is spontaneosuly broken at a certain scale Λ_t.
The strong dynamics leads to the formation of a large top quark condensate (tb) and explain for its big mass.

Flavour changing neutral currents (I)

- **Single top sensitivity to Beyond Standard Model (BSM) physics**

EXTRA COUPLINGS

Top color assisted technicolor
MSSM, ~~R~~ SUSY …

⇨

flavor changing neutral currents
at detectable rates

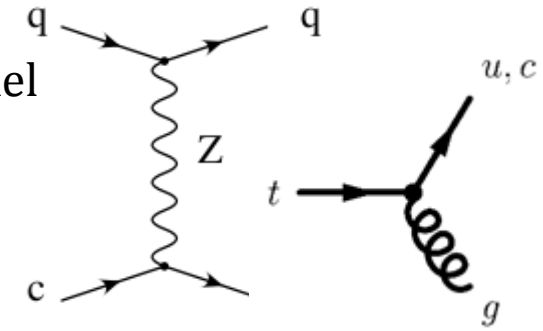

- t-channel — cross section increased as PDF(u/c)>PDF(b) in the incoming quark
- s-channel & Wt production — exotic production mechanisms but different final states
- all single top rates — could be enhanced by open top decay channels to light quarks

Flavour changing neutral currents (II)

Theoretical values for the branching fractions of FCNC top quark decays as predicted by

Process	SM	2HDM II	2HDM III	MSSM	$\not{R}$ SUSY	Extra q	TC2
$t \to u\gamma$	3.7×10^{-16}	—	—	2×10^{-6}	1×10^{-6}	—	—
$t \to uZ$	8×10^{-17}	—	—	2×10^{-6}	3×10^{-5}	—	—
$t \to ug$	3.7×10^{-14}	—	—	8×10^{-5}	2×10^{-4}	—	—
$t \to c\gamma$	4.6×10^{-14}	$\sim 10^{-7}$	$\sim 10^{-7}$	2×10^{-6}	1×10^{-6}	$\sim 10^{-8}$	$\sim 10^{-7}$
$t \to cZ$	$\sim 1 \times 10^{-14}$	$\sim 10^{-8}$	$\sim 10^{-6}$	2×10^{-6}	3×10^{-5}	$\sim 10^{-4}$	$\sim 10^{-5}$
$t \to cg$	4.6×10^{-12}	$\sim 10^{-5}$	$\sim 10^{-4}$	8×10^{-5}	2×10^{-4}	$\sim 10^{-7}$	$\sim 10^{-5}$

SM

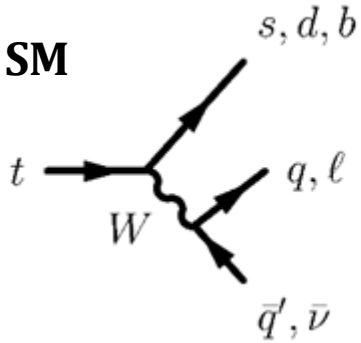

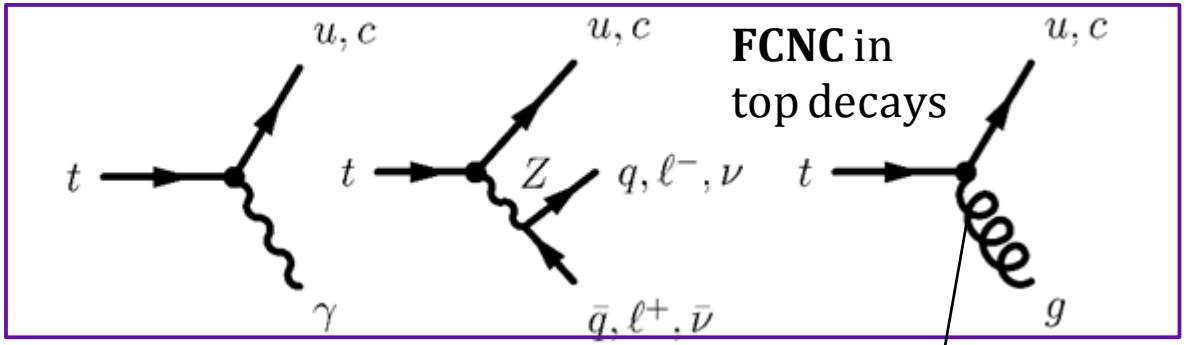

FCNC in top decays

t-g-q coupling better studied in production mechanism, since final state signatures dominated by multijet background

σ (qg→t)x B(t →Wb)<2.5 pb ATLAS-CONF-2013-063

Extra quarks (I)

- **Single top sensitivity to Beyond Standard Model (BSM) physics**

EXTRA QUARKS

Top color assisted technicolor
top flavor, SUSY …

⇨

additional chiral family
of fermions

- all single top channels

modified cross sections
since V_{tb} could deviate from 1
(mixing effect)

- t-channel & s-channel

increased rates if b' is directly
produced and decays into b

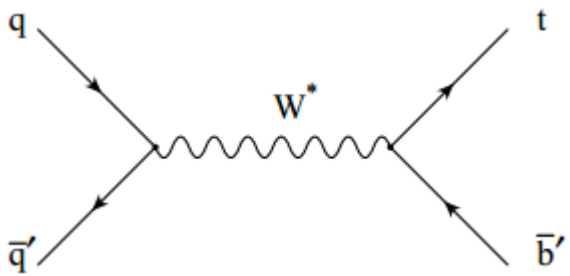

Extra quarks (II)

Fourth generation of fermions arXiv:1204.1252, 2012

- H →γγ signal above SM expectation [ATLAS & CMS]
  while the rate predicted by SM4 is below
- Higgs-strahlung channel above SM expectation [D0 & CDF]
  while the rate predicted by SM4 is below
- H→ττ is not enhanced as SM4 estimates

Vector like quarks Phys. Rev. D 88,2013

"hypothetical spin 1/2 particles that transform as triplets under the color gauge group and whose left- and right-handed components have the same color and electroweak quantum numbers"

Direct production
Small deviations in V_{tb},

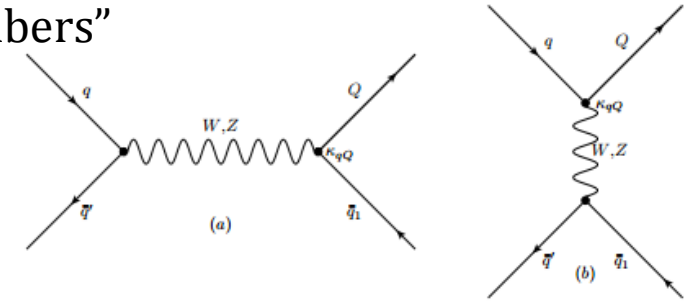

Single top interference

s and t channels at the NLO

Take $ug \longrightarrow t\bar{b}d$:

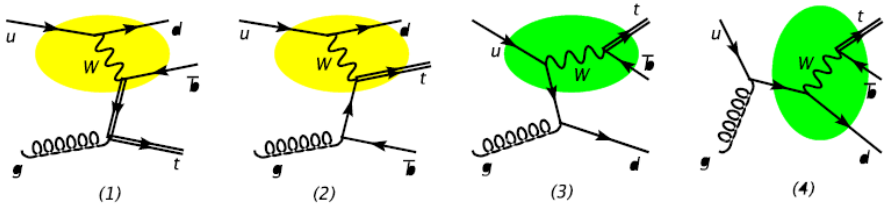

- Same initial and final states: s- and t-channel contributions interfere
- The day is saved by the fact that the interference is zero $(\mathrm{Tr}(\lambda^a) = 0)$
- At the next order, this is not longer the case

As for Wt...

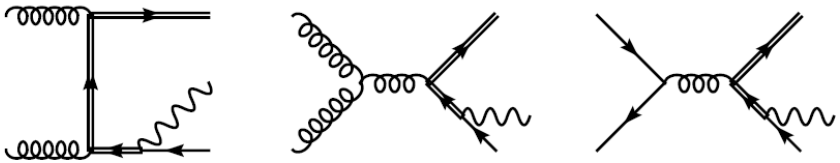

One just can't tell whether these diagrams are relevant to $t\bar{t}$ (with the t decay not drawn) or to Wt production

- $t\bar{t}$ and Wt production *interfere* at $\mathcal{O}(\alpha_W \alpha_s^2)$

Again, Wt production can be defined only in an operative manner
(Laenen, Motylinski, Webber, White, SF, 2008) $\longrightarrow$

DR: *Diagram removal:* eliminate all doubly-resonant diagrams

DS: *Diagram subtraction:* subtract locally $t\bar{t}$ contributions

PR: *Process removal:* do not include the contributions from processes which interfere with $t\bar{t}$

Stefano Frixione
Single-top theory
SM@LHC, Madrid, 10/4/2014

B-tagging

$$w_{jet} = \sum_{i=1}^{N_T} ln \frac{b(X_i)}{u(X_i)};$$

Likelihood ratio to compare the measured value of a discriminating variable Xi to reference MC distributions obtained for light- and b-jets.

Different cut-values on the jet weight → several **working points**:

- b-tagging efficiency
- light/c mistagging rates (prob of mis/c-tagging) $^{-1}$

∀ w.p. **calibration with data** → p_T-dependent SF $k_{\epsilon_b}^{data/MC} = \frac{\epsilon_b^{data}}{\epsilon_b^{MC}}$.

- via jets containing muons:
  -- p_T rel : template fit of muon p_T respect to jet axis ($p_{T\,rel}$) to get flavor fraction before and after b-tagging
  -- System8: 3 independent jet selection criteria to construct 8 samples. B-tagging efficiency extracted from the different event yields

→ Results combined to improve scale factor precision

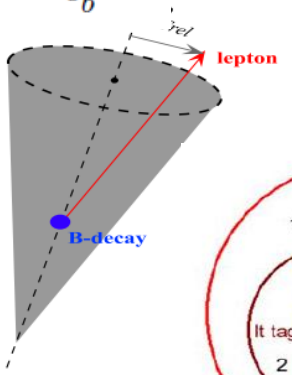

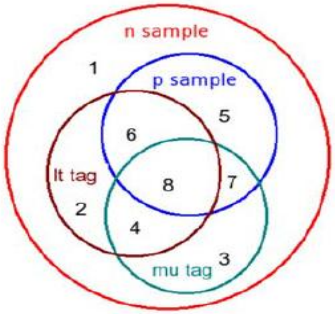

- via top pairs (dilepton & single lepton) for high p_T range

B-tagging algorithms (I)

IP3D: transverse and longitudinal impact parameter significance as the PDFs

SV1: reconstructs secondary vertex and take likelihood ratio of:
invariant mass, (p_T SV track)/(p_T all tracks in jet) ,
n. of two-track vertices, ΔR (jet-direction, line joining PV & SV)

JetFitter: exploits the topology of weak B/C-hadron decay chain (b → c → X) inside jets and employs a Kalman filter to find a common line on
PV → b vertex → c vertex decay chain

JetFitterCombNN: combination of JetFitter & IP3D & topological variables based on artificial neural network techniques (MC training)

MV1: neural network tagger exploiting JetFitterCombNN, JetFitter, SV1 as input

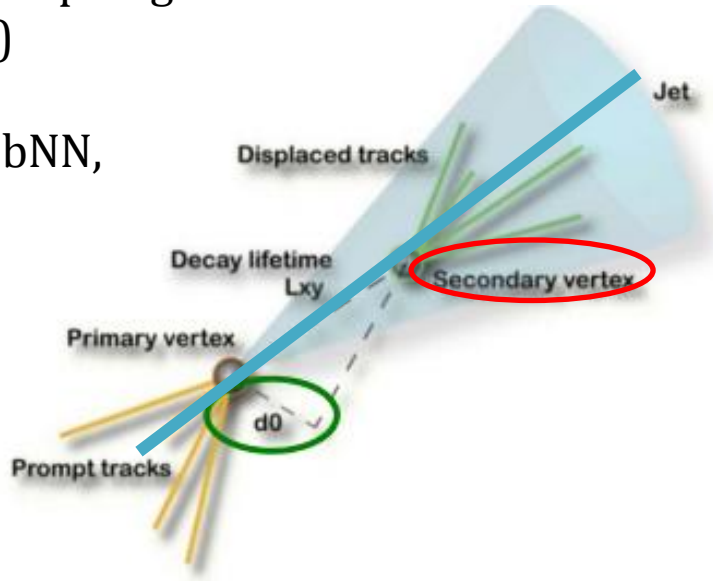

B-tagging algorithms (II)

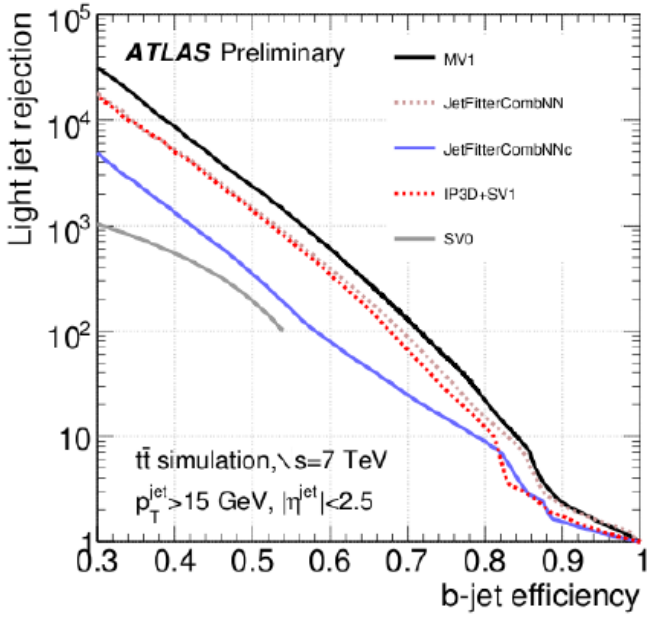

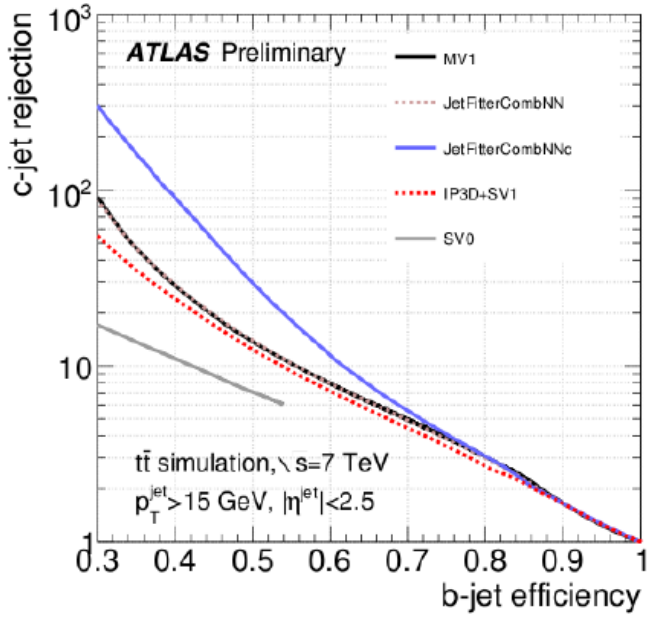

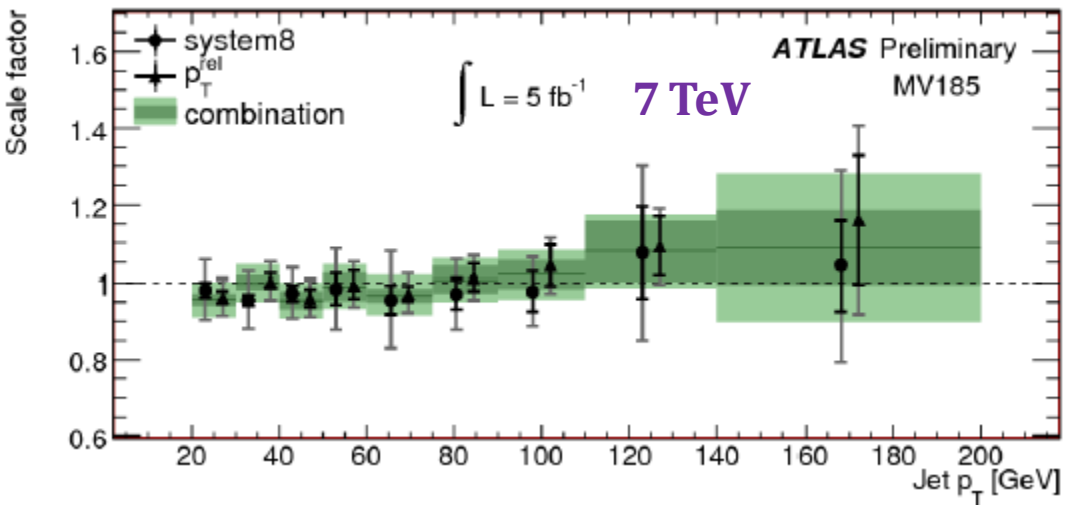

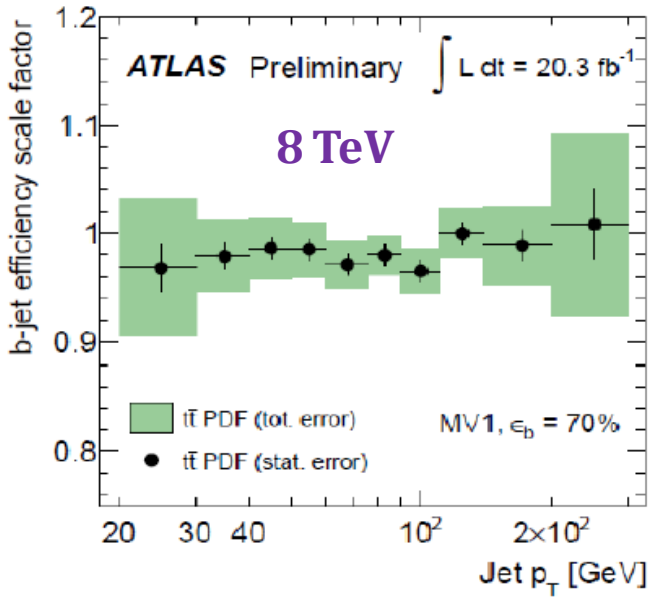

Matrix method parametrization (I)

$\varepsilon_{real/fake}$ is η-dependent, but in case of significant dependence on other variables → further parametrization: $\epsilon_{fake} = \epsilon_{fake}(\eta) \cdot \frac{f(x)}{< \epsilon_{fake} >}$.

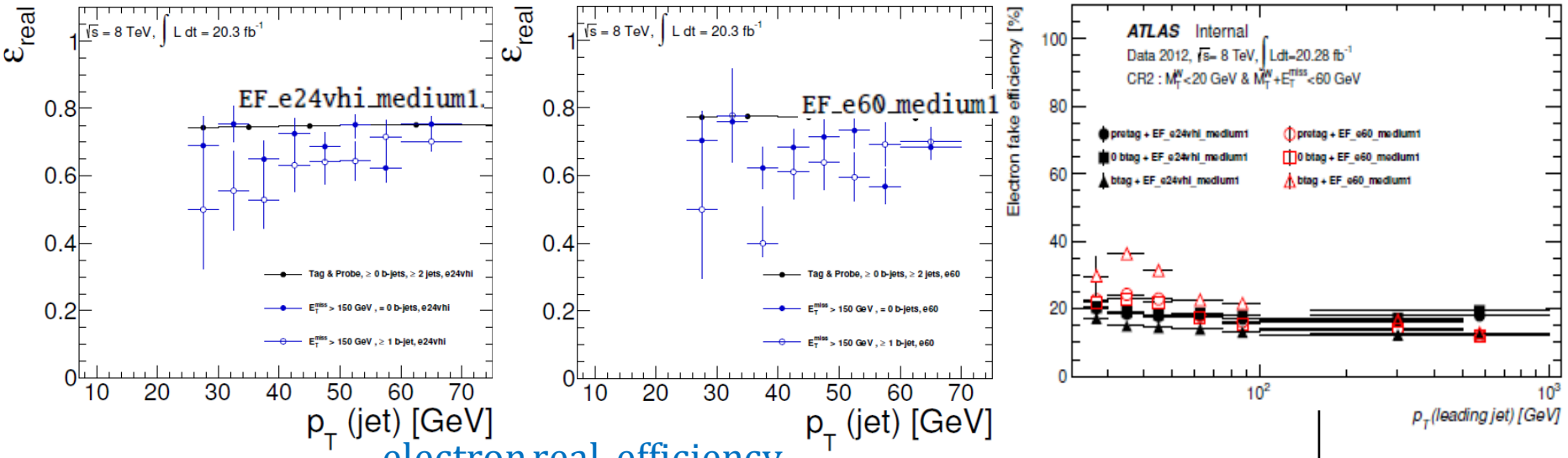

electron real efficiency

- Tag&Probe: parametrization in η and 2 jet-multiplicity bins
- high MET: ε= ε[η(l)] x ε[pt(j1)]/<ε> x ε[min(ΔR(l,j))]/<ε>

electron fake efficiency

- parametrization A: 3D, as function of Et and η electron, pT(j1)/ ΔR(j1,l)
- parametrization B: same variables than A but treated as uncorrelated

Matrix method parametrization (II)

$\varepsilon_{real/fake}$ is η-dependent, but in case of significant dependence on other variables → further parametrization: $\epsilon_{fake} = \epsilon_{fake}(\eta) \cdot \frac{f(x)}{< \epsilon_{fake} >}$.

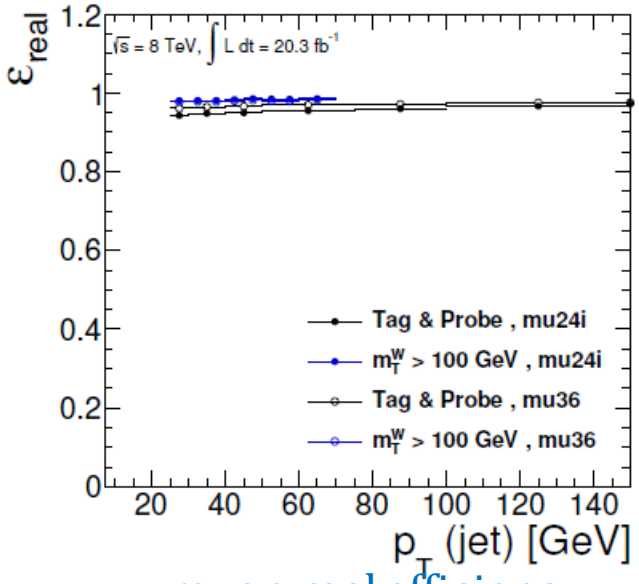

muon real efficiency

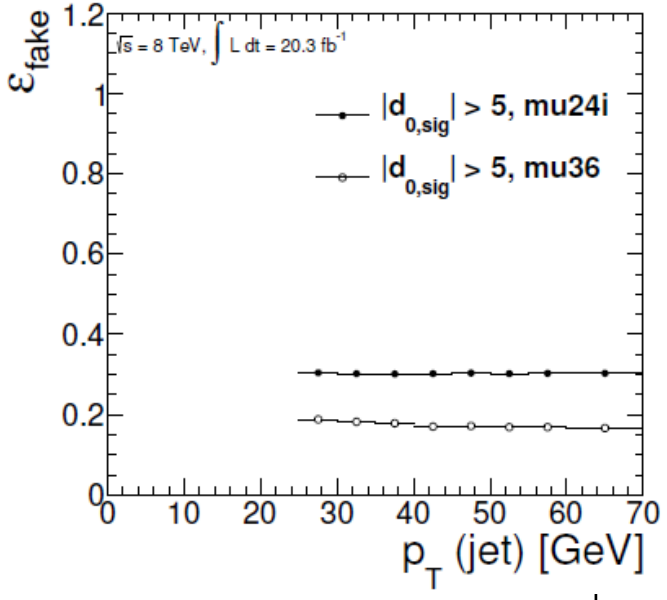

- Tag&Probe: ε= ε[η(l)] x ε[Et(l)]/<ε> x ε[pT(closest j)/ΔR(j,l))]/<ε>
- high MTW: ε= ε[η(l)] x ε[pt(j1)]/<ε> x ε[min(ΔR(l,j))]/<ε>

muon fake efficiency

parametrization: ε= ε[η(clust)] x ε[pt(l)]/<ε> x ε[min(ΔR(l,j))]/<ε>

Boosted decision trees

Splitting criterion: algorithm core, based on the maximization of a figure of merit representing the decrease of impurity *i* for the split *S* into the daughters t_f, t_p

$$\Delta_i(S,t) = i(t) - p_p i(t_p) - p_f i(t_f), \quad i(t) = Gini = \frac{2sb}{(s+b)^2}$$

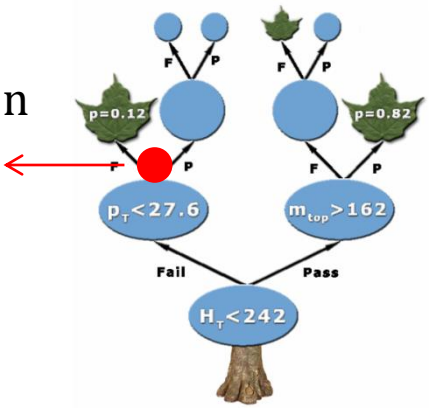

Boosting algorithm: maximizes the generalization potential by associating higher weights to the events misclassified by the first classifier, overwhelms the shortcoming of discrete output.

BDT output

n. of DT (weak learners)

Boosting weight for m

Learning rate of boosting algorithm

$$F(\mathbf{x}; P) = \sum_{m=0}^{M} \beta_m f(\mathbf{x}, a_m), \quad P \in \{\beta_m, a_m\}_0^M$$

Parameters which minimize the difference between the model response F(x) and the true value y, modelled by loss function:

gradient boost algorithm $\longrightarrow$ $L(F,y) = ln(1 + e^{-2F(\mathbf{x})}y)$

Expected CLs (I)

Limit setting

- Q_1= median value Q distribution obtained for the S+B ensemble
- p_b= $P(Q<Q_1 \mid B)$

- Q_0= median value Q distribution obtained for the B only ensemble
- p_{s+b}= $P(Q>Q_0 \mid S+B)$

- Signal hypothesis (n. times SM) is excluded at 95% CL
  if $CL_s = p_{s+b}/(1-p_b)<5\%$

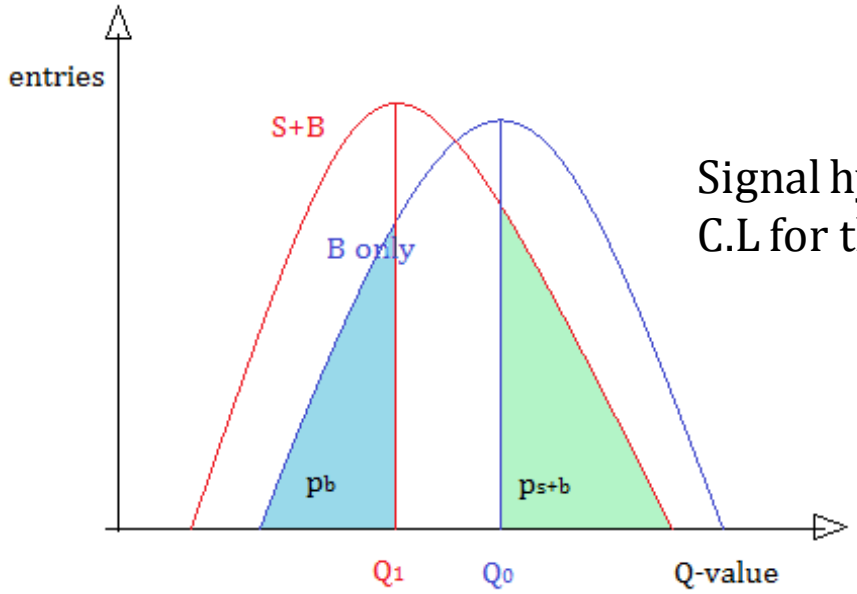

Signal hypothesis defined as the fraction of C.L for the S+B and B hypotheses

Expected CLs (II)

Limit setting

- Q_1= median Q value, B+S ensemble
- p_b= P(Q<Q_1 | B)

- Q_0= median Q value, B only ensemble
- p_{s+b}= P(Q>Q_0 | S+B)

→ CLs= $p_{s+b}/(1-p_b)$<5% for

observed(S+B, B only)

ATLAS: 14.6 (15.7, 9.4) pb
CMS: 11.5 (17.0, 9.0) pb

Signal hypothesis

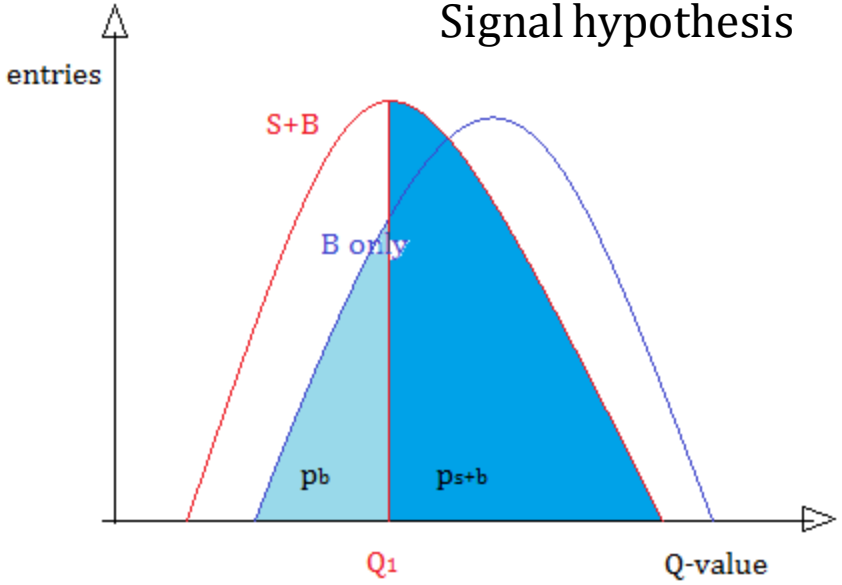

Background only hypothesis

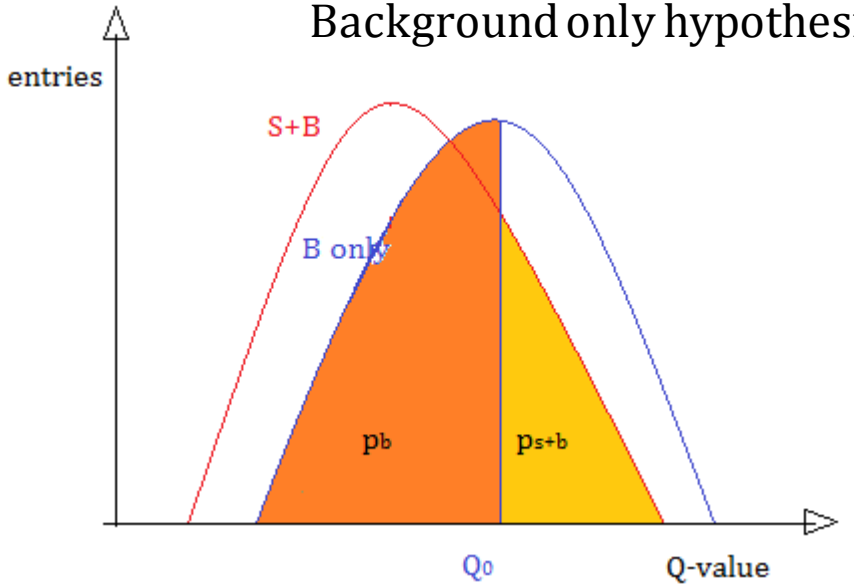

Selection cuts

7 TeV ANALYSIS

Preselection

Lepton pt>25 GeV
Jets pt> 30 GeV, b-tagging with MV1 85%
MET>30 GeV
MTW>30 GeV

Signal selection

2 b-tag jets, cut on BDT(tt)

W+jets enriched samples

1 b-tag jet

Top pairs enriched sample

3 jets, 2 of which b-tag

8 TeV ANALYSIS

Preselection

Lepton pt>30 GeV
Jets pt> 30 GeV
MET>35 GeV
MTW>30 GeV

Signal selection

2 b-tag jets, MV1 70%
Top jet pt>50 GeV
MTW>50 GeV

W+jets enriched samples

2 b-tag jets with pt>25 GeV, MV1 80%

Top pairs enriched sample

4 b-tag jets with pt>25 GeV, MV1 80

7 TeV dataset

Data collected in 2011, integrated luminosity: 4.7 fb^{-1}

Signal and background estimations

MC simulations implementing theoretical cross sections:

- Single top
- Top pair
- Z+jets & Diboson

Data-driven approach:

- W+jets normalization via tag & counting method (rescaling of specific MC samples)
- Multijet
  electron+jets final state: jet-electron model
  muon+jets: matrix method

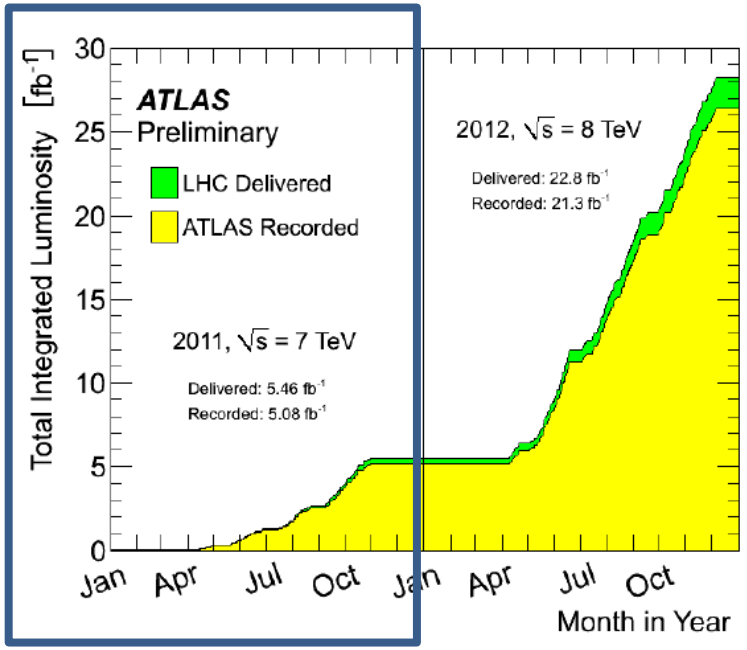

7 TeV strategy

Preselection: common cuts detailed before

W+jets enriched region	Signal-enriched region	Top pair-enriched region
1 b-jet	2 b-jets	3 jets, 2 of which b-tag

Boosted decision trees

W+jets discrimination

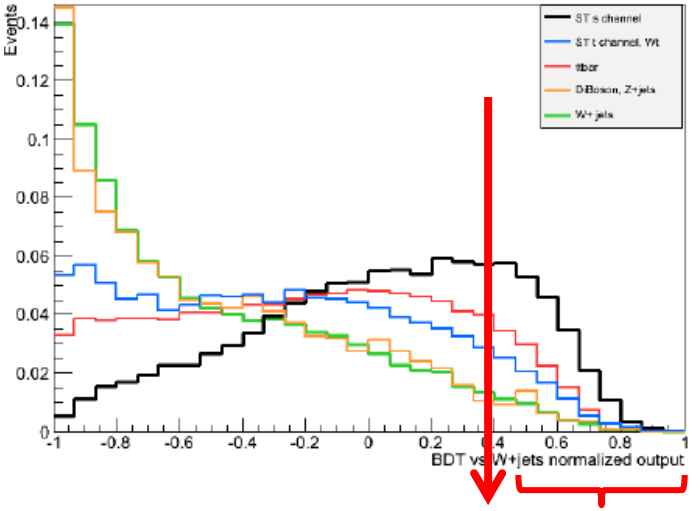

Top pairs discrimination

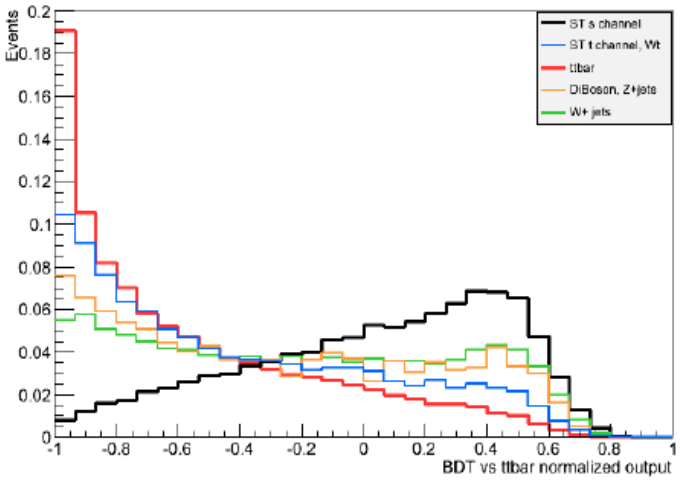

Signal selection

Threshold value on BDT_{W+jets} optimizing total s-channel cross section uncertainty and CLs limit → signal purity increases from 1.4 to 4.6 %

7 TeV input variables BDT_{W+jets}

Variable	S
$\Delta\eta(l,j1)$	0.139
$p_T(j2)$	0.138
$Ht(j1,j2)$	0.136
$\Delta\eta(t2,j1)$	0.112
$\Delta\eta(t1,j2)$	0.106
$\Delta R(l,j1)$	0.105
$\Delta\eta(j1,j2)$	0.104
$p_T(Top_j1\nu l)$	0.103
H_T	0.098
$p_T(Top_j2\nu l)$	0.096
$P_T(l,j1)$	0.096
$Whelicity_j1\nu l$	0.095
$\Delta\Phi(t1,j2)$	0.091
$m(Top_j1\nu l)$	0.088
$E_T(l)$	0.087
$Centrality$	0.083
$\Delta\Phi(t2,j1)$	0.077
$Sphericity$	0.073
$E(j2)$	0.072
$m(j1,j2)$	0.066
$E_T(j1,j2)$	0.066
$cos\theta(Top_j2\nu l)$	0.062
$m(l,j2)$	0.062
$Whelicity_j2\nu l$	0.061
$m(l,j1)$	0.058
$m(Top_j2\nu l)$	0.053
$Aplanarity$	0.051

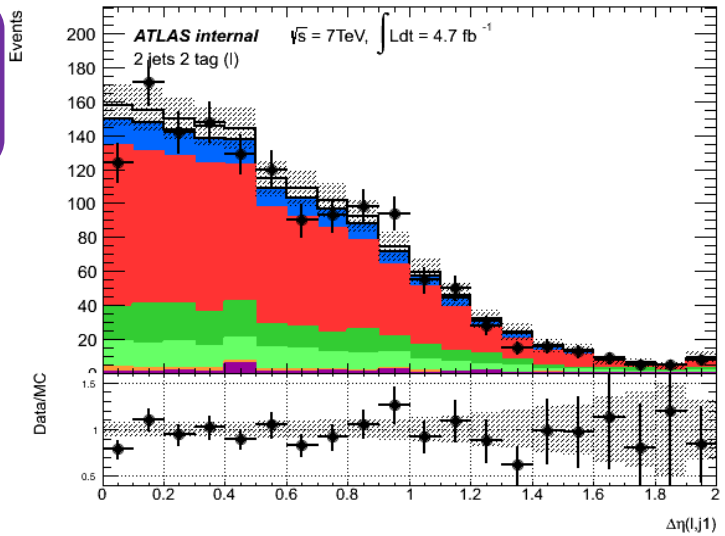

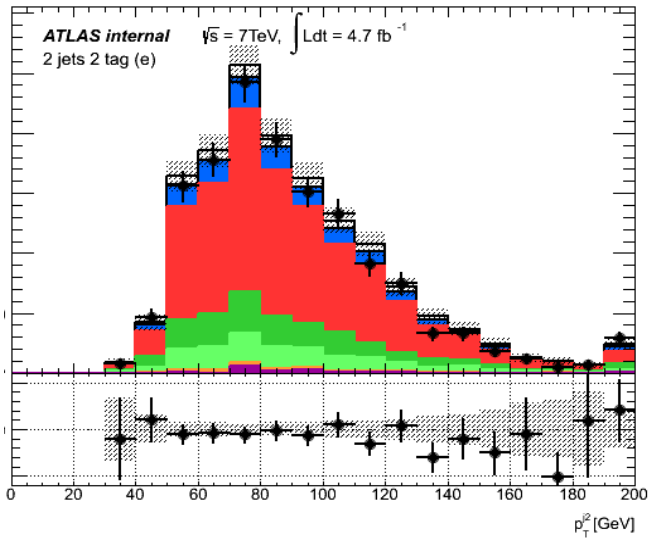

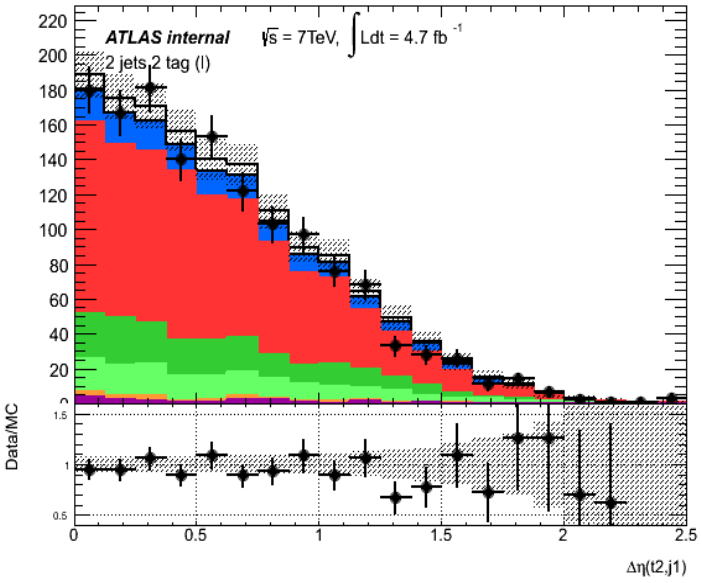

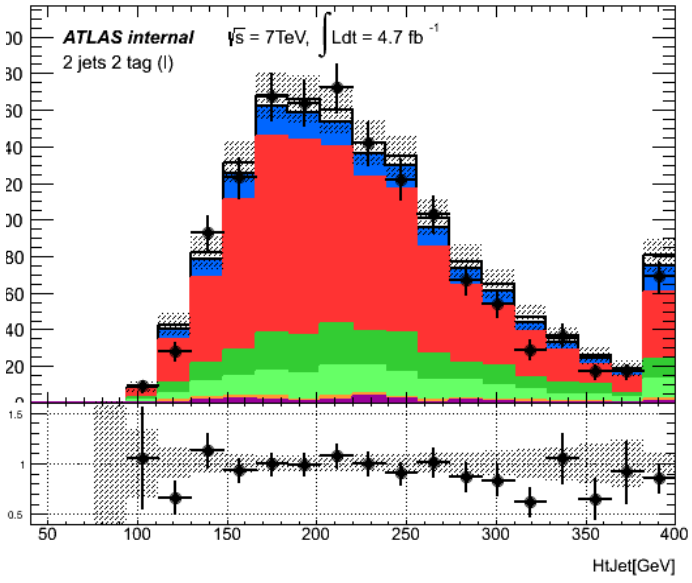

7 TeV input variables BDT_{ttbar}

Variable	S
$p_T(l,\nu,j1,j2)$	0.215
$\Delta\Phi(t1,j2)$	0.193
$\Delta\Phi(t2,j1)$	0.178
$p_T(l)+E_T^{miss}$	0.159
E_T^{miss}	0.125
$m(Top_j2\nu l)$	0.089
$\Delta\Phi(j1,j2)$	0.089
$p_T(l)$	0.085
$m_T(W)$	0.084
$\eta(j1,j2)$	0.081
$H_T(j1,j2)$	0.081
$m(Top_j1\nu l)$	0.075
$m(l,j2)$	0.073
$m(l,\nu,j1,j2)$	0.069
$\Delta R(j1,j2)$	0.063
$\eta(l,j1)$	0.063
$m(l,j1)$	0.061
$\Delta\Phi(j2,E_T^{miss})$	0.059
$\Delta\eta(t2,j1)$	0.051

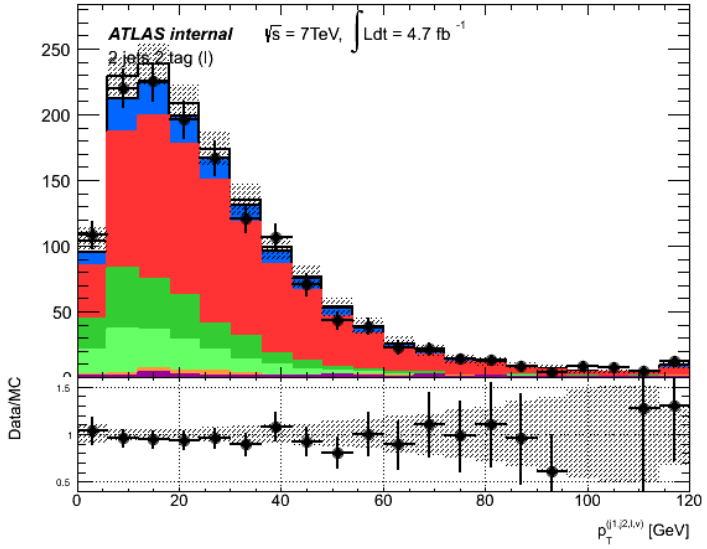

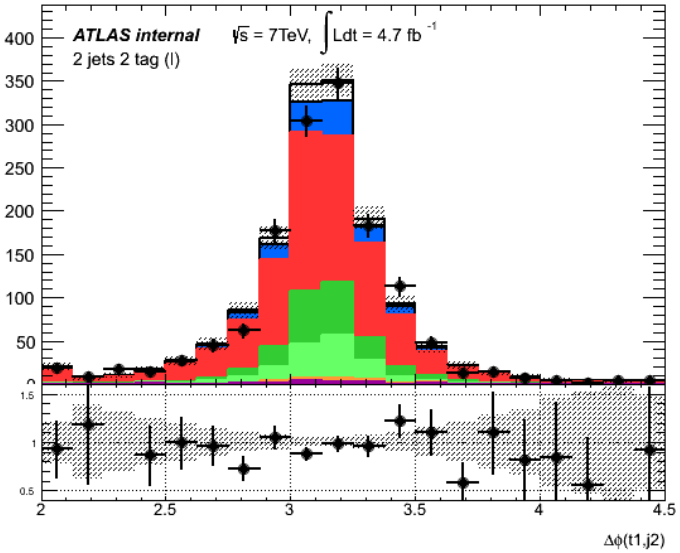

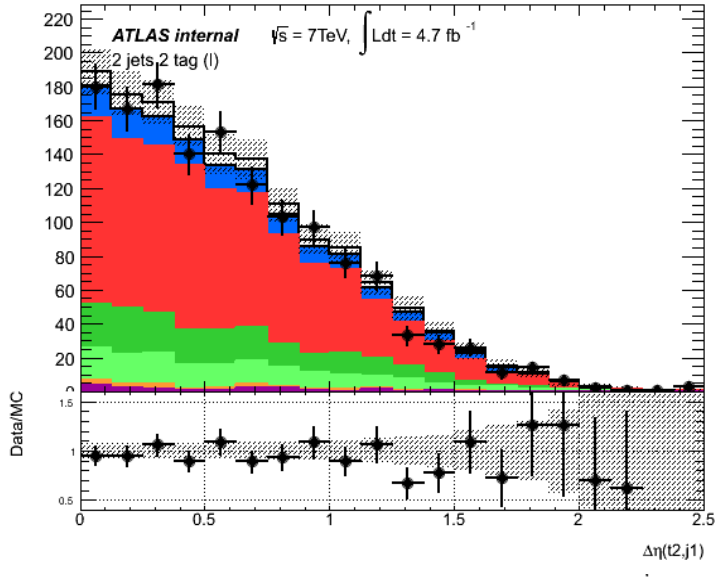

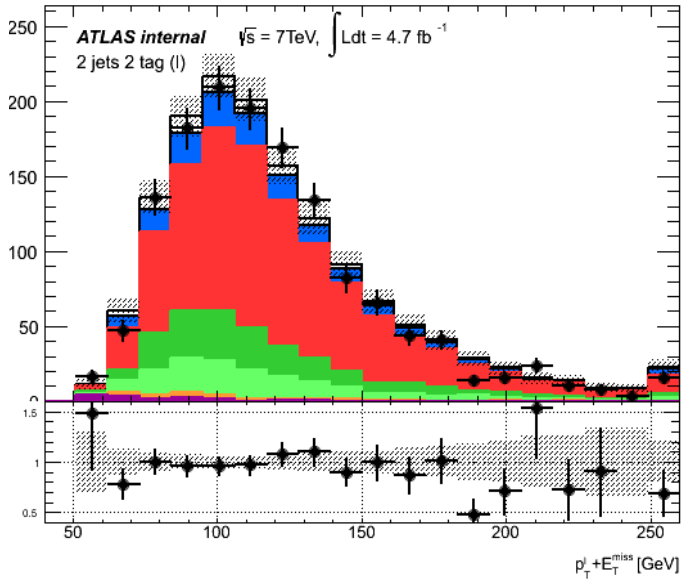

7 TeV likelihood fit

After the event selection, analysis sensitivity still very low…

Statistical fluctuations and total uncertainty on the expected cross section reduced with a **simultaneous fit** of:

a) **m_T(W)** in the 1-jet bin ⟶ constrain W+jets events

b) **BDTttbar** in the 2-jets bin signal region ⟶ extract s-channel contribution

c) **vectorial sum of final particles pt** in the 3-jets bin ⟶ constrain ttbar events

σ_s

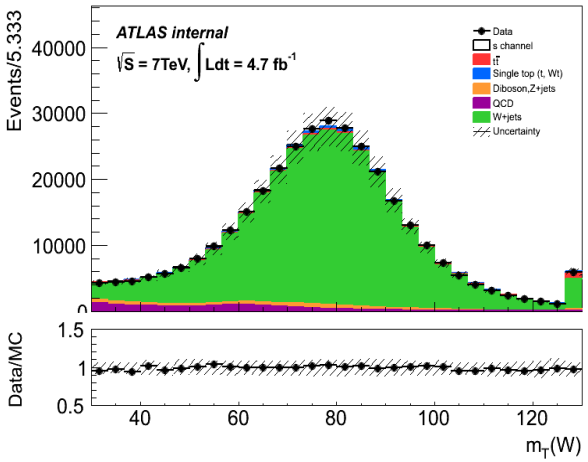

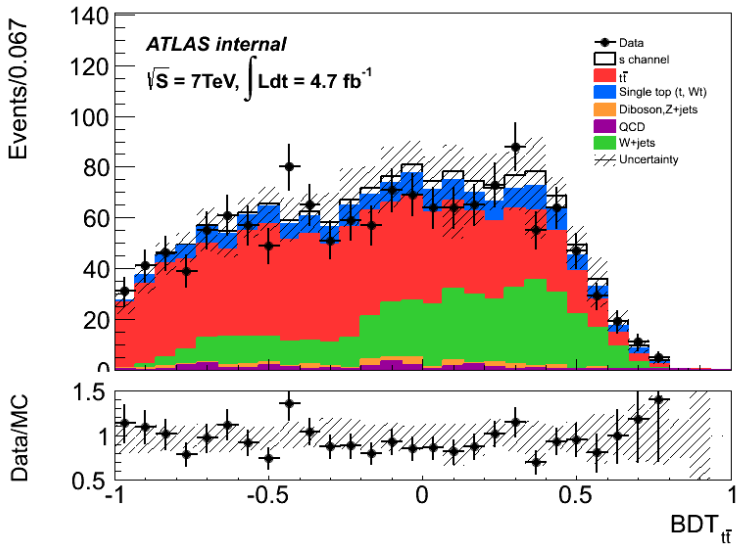

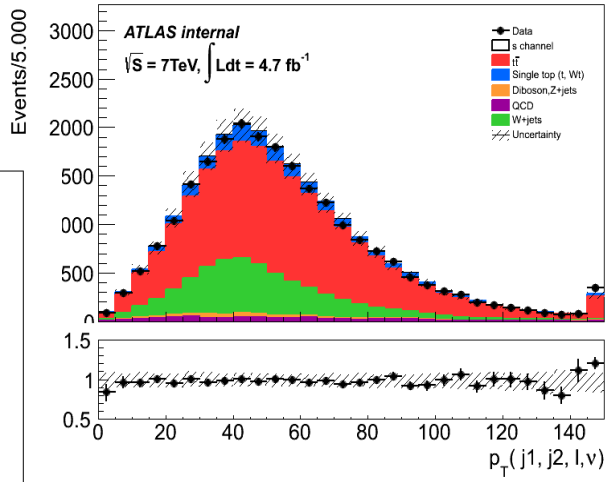

7 TeV results

Cross section uncertainty

Total expected uncertainty:
+153%, -168%

Dominant contribution from
- jet energy scale (89%)
- E_T^{miss} scale and resolution (56%)
- b-tag efficiency (52%)

Significance & limit calculation

Single top s-channel production excluded only if its cross section is greater than 4.7 times the SM one:

$\sigma_s < 21.7$ (14.3 exp) pb at 95% C.L

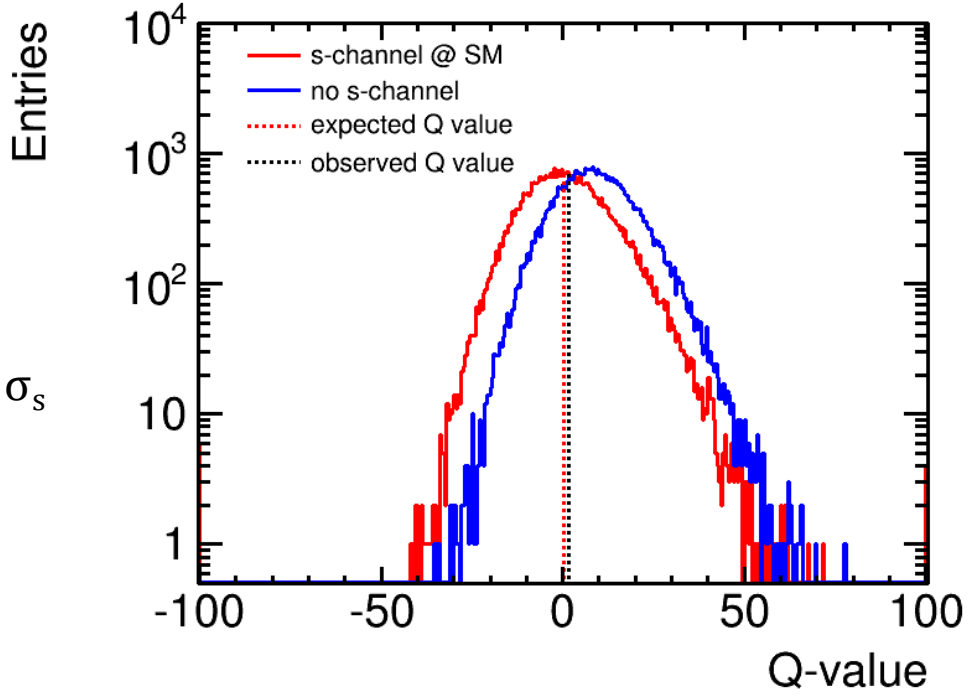

cross section measurement sensitivity: 0.6 standard deviations (0.8 expected)

8 TeV dataset

Sample	Generator	σ [pb]	N_{events}
s-channel (l+jets)	POWHEG+PYTHIA6	1.8	1 199 895
Wt (DR)	POWHEG+PYTHIA6	22.3	999 692
t-channel (l+jets, t)	POWHEG+PYTHIA6	18.4	2 994 591
t-channel (l+jets, $\bar{t}$)	POWHEG+PYTHIA6	9.9	1 999 888
$t\bar{t}$ (no full-had.)	POWHEG+PYTHIA6	137.3	14 996 424
$t\bar{t}$ (no full-had.)	POWHEG+HERWIG	137.3	29 960 959
$t\bar{t}$ (no full-had.)	MC@NLO+HERWIG	137.3	14 997 103
$t\bar{t} \rightarrow l\nu l\nu$ + 0 parton	ALPGEN+HERWIG	8.3	799 897
$t\bar{t} \rightarrow l\nu l\nu$ + 1 partons	ALPGEN+HERWIG	8.8	808 897
$t\bar{t} \rightarrow l\nu l\nu$ + 2 partons	ALPGEN+HERWIG	5.7	529 996
$t\bar{t} \rightarrow l\nu l\nu$ + 3 partons	ALPGEN+HERWIG	3.8	359 997
$t\bar{t} \rightarrow l\nu qq$ + 0 parton	ALPGEN+HERWIG	34.5	3 359 080
$t\bar{t} \rightarrow l\nu qq$ + 1 partons	ALPGEN+HERWIG	36.5	3 398 787
$t\bar{t} \rightarrow l\nu qq$ + 2 partons	ALPGEN+HERWIG	23.5	2 209 980
$t\bar{t} \rightarrow l\nu qq$ + 3 partons	ALPGEN+HERWIG	15.7	1 459 791
Wt (DS)	POWHEG+PYTHIA6	22.3	999 995
Wt	MC@NLO+HERWIG	22.3	1 999 194
t-channel (l+jets)	aMC@NLO+HERWIG	28.3	999 896
s-channel (e+jets)	MC@NLO+HERWIG	0.6	199 997
s-channel (μ+jets)	MC@NLO+HERWIG	0.6	200 000
s-channel (τ+jets)	MC@NLO+HERWIG	0.6	199 999
$t\bar{t}$ (no full-had., more PS)	ACERMC+PYTHIA6	137.3	14 985 986
$t\bar{t}$ (no full-had., less PS)	ACERMC+PYTHIA6	137.3	14 988 492

Sample	Generator	σ [pb]	N_{events}
$Z \rightarrow ee$ + 0 parton	ALPGEN+PYTHIA6	848.4	6 298 988
$Z \rightarrow ee$ + 1 partons	ALPGEN+PYTHIA6	207.3	8 169 476
$Z \rightarrow ee$ + 2 partons	ALPGEN+PYTHIA6	69.5	3 175 991
$Z \rightarrow ee$ + 3 partons	ALPGEN+PYTHIA6	18.4	894 995
$Z \rightarrow ee$ + 4 partons	ALPGEN+PYTHIA6	4.7	398 597
$Z \rightarrow ee$ + 5 partons	ALPGEN+PYTHIA6	1.5	229 700
$Z \rightarrow \mu\mu$ + 0 parton	ALPGEN+PYTHIA6	848.6	6 298 796
$Z \rightarrow \mu\mu$ + 1 partons	ALPGEN+PYTHIA6	206.7	8 188 384
$Z \rightarrow \mu\mu$ + 2 partons	ALPGEN+PYTHIA6	69.5	3 175 488
$Z \rightarrow \mu\mu$ + 3 partons	ALPGEN+PYTHIA6	18.5	894 799
$Z \rightarrow \mu\mu$ + 4 partons	ALPGEN+PYTHIA6	4.7	388 200
$Z \rightarrow \mu\mu$ + 5 partons	ALPGEN+PYTHIA6	1.5	229 200
$Z \rightarrow \tau\tau$ + 0 parton	ALPGEN+PYTHIA6	848.3	19 352 765
$Z \rightarrow \tau\tau$ + 1 partons	ALPGEN+PYTHIA6	207.4	10 669 582
$Z \rightarrow \tau\tau$ + 2 partons	ALPGEN+PYTHIA6	69.5	3 710 893
$Z \rightarrow \tau\tau$ + 3 partons	ALPGEN+PYTHIA6	18.5	1 091 995
$Z \rightarrow \tau\tau$ + 4 partons	ALPGEN+PYTHIA6	4.7	398 798
$Z \rightarrow \tau\tau$ + 5 partons	ALPGEN+PYTHIA6	1.5	229 799
$W \rightarrow e\nu$ + 0 parton	ALPGEN+PYTHIA6	9 208.2	29 434 220
$W \rightarrow e\nu$ + 1 partons	ALPGEN+PYTHIA6	2 031.1	48 155 904
$W \rightarrow e\nu$ + 2 partons	ALPGEN+PYTHIA6	614.3	17 554 347
$W \rightarrow e\nu$ + 3 partons	ALPGEN+PYTHIA6	167.3	4 985 287
$W \rightarrow e\nu$ + 4 partons	ALPGEN+PYTHIA6	42.8	2 548 292
$W \rightarrow e\nu$ + 5 partons	ALPGEN+PYTHIA6	13.6	799 192
$W \rightarrow \mu\nu$ + 0 parton	ALPGEN+PYTHIA6	9 208.0	31 965 655
$W \rightarrow \mu\nu$ + 1 partons	ALPGEN+PYTHIA6	2 031.4	43 677 615
$W \rightarrow \mu\nu$ + 2 partons	ALPGEN+PYTHIA6	614.4	17 611 454
$W \rightarrow \mu\nu$ + 3 partons	ALPGEN+PYTHIA6	166.8	4 956 077
$W \rightarrow \mu\nu$ + 4 partons	ALPGEN+PYTHIA6	42.7	2 546 595
$W \rightarrow \mu\nu$ + 5 partons	ALPGEN+PYTHIA6	13.6	788 898
$W \rightarrow \tau\nu$ + 0 parton	ALPGEN+PYTHIA6	9 208.0	31 902 157
$W \rightarrow \tau\nu$ + 1 partons	ALPGEN+PYTHIA6	2 030.6	48 255 178
$W \rightarrow \tau\nu$ + 2 partons	ALPGEN+PYTHIA6	614.4	17 581 943
$W \rightarrow \tau\nu$ + 3 partons	ALPGEN+PYTHIA6	167. 2	4 977 982
$W \rightarrow \tau\nu$ + 4 partons	ALPGEN+PYTHIA6	42.8	2 548 295
$W \rightarrow \tau\nu$ + 5 partons	ALPGEN+PYTHIA6	13.6	789 096
$W \rightarrow l\nu + b\bar{b}$ + 0 parton	ALPGEN+PYTHIA6	63.1	1 599 997
$W \rightarrow l\nu + b\bar{b}$ + 1 partons	ALPGEN+PYTHIA6	51.3	1 398 396
$W \rightarrow l\nu + b\bar{b}$ + 2 partons	ALPGEN+PYTHIA6	27.3	699 398
$W \rightarrow l\nu + b\bar{b}$ + 3 partons	ALPGEN+PYTHIA6	12.7	398 397
$W \rightarrow l\nu + c\bar{c}$ + 0 parton	ALPGEN+PYTHIA6	170.2	4 299 592
$W \rightarrow l\nu + c\bar{c}$ + 1 partons	ALPGEN+PYTHIA6	150.3	3 987 891
$W \rightarrow l\nu + c\bar{c}$ + 2 partons	ALPGEN+PYTHIA6	81.4	2 394 394
$W \rightarrow l\nu + c\bar{c}$ + 3 partons	ALPGEN+PYTHIA6	32.3	985 295
$W \rightarrow l\nu + c$ + 0 parton	ALPGEN+PYTHIA6	1228.2	22 769 047
$W \rightarrow l\nu + c$ + 1 partons	ALPGEN+PYTHIA6	406.9	8 198 769
$W \rightarrow l\nu + c$ + 2 partons	ALPGEN+PYTHIA6	106.2	2 090 290
$W \rightarrow l\nu + c$ + 3 partons	ALPGEN+PYTHIA6	31.3	499 498
$W \rightarrow l\nu + c$ + 4 partons	ALPGEN+PYTHIA6	6.6	199 499
WW	HERWIG	20.9	2 499 890
ZZ	HERWIG	1.5	245 000
WZ	HERWIG	7.0	999 998

8 TeV BDT input variables (II)

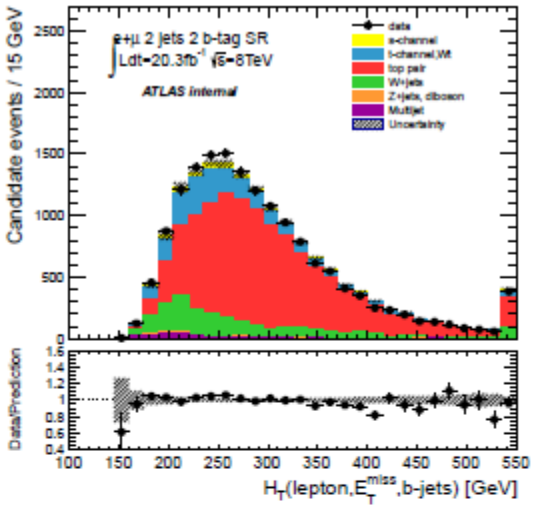

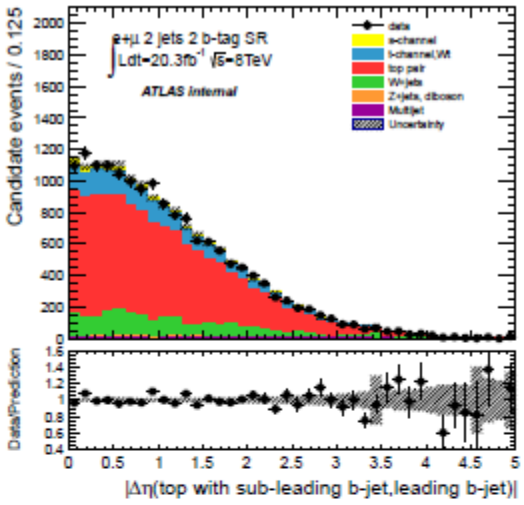

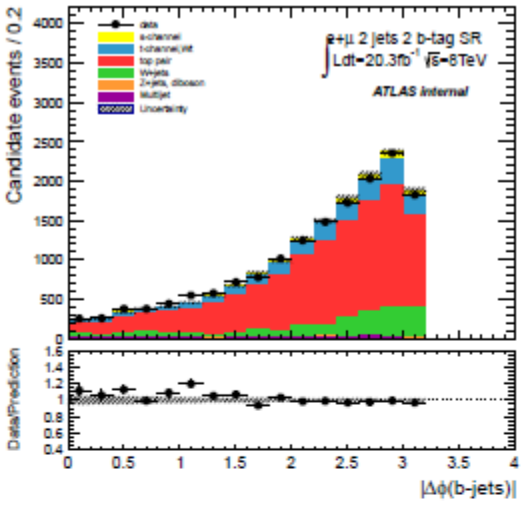

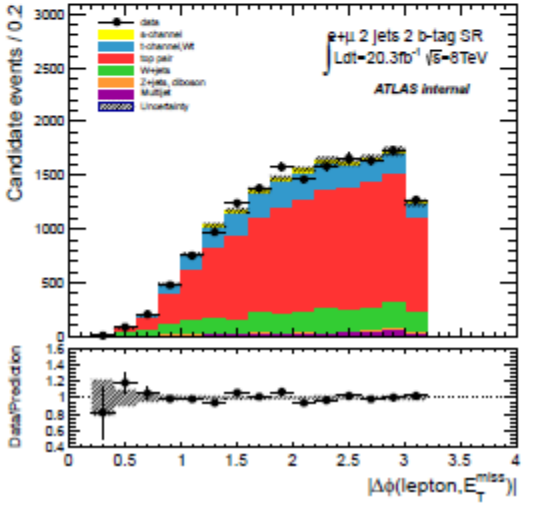

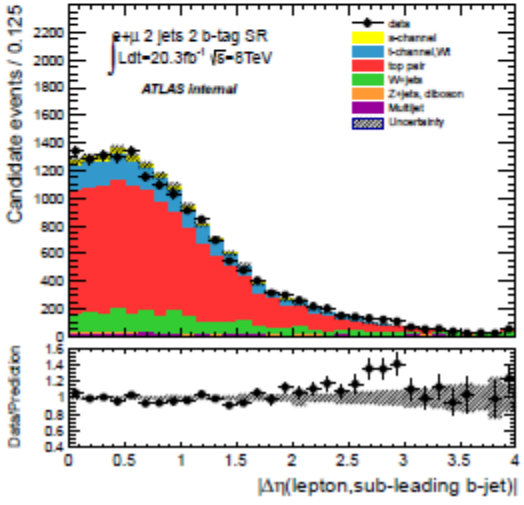

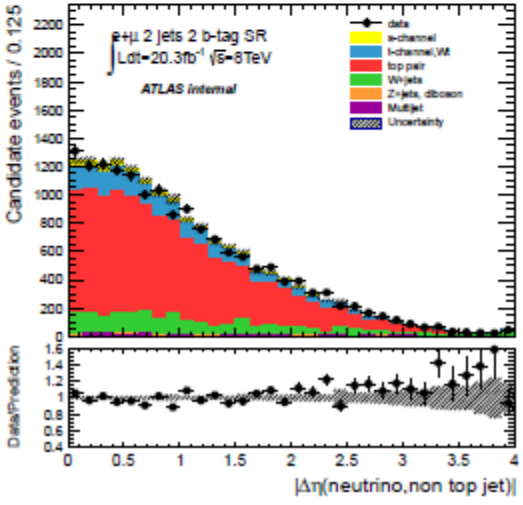

8 TeV BDT input variables (III)

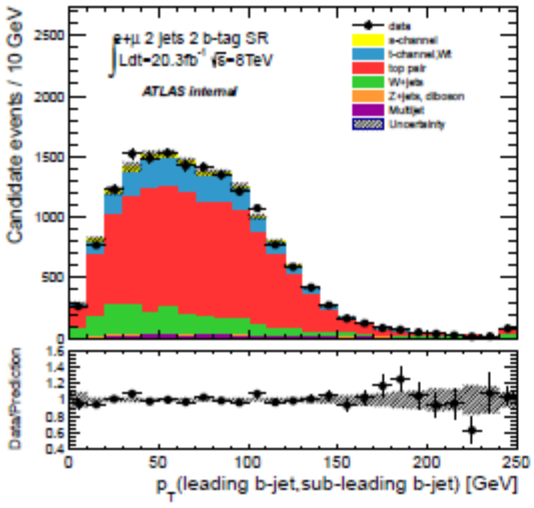

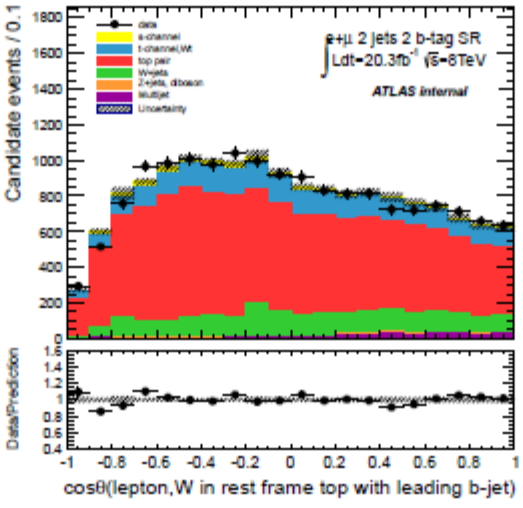

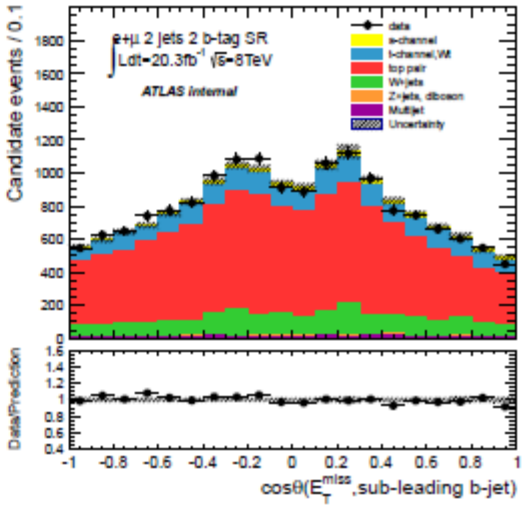

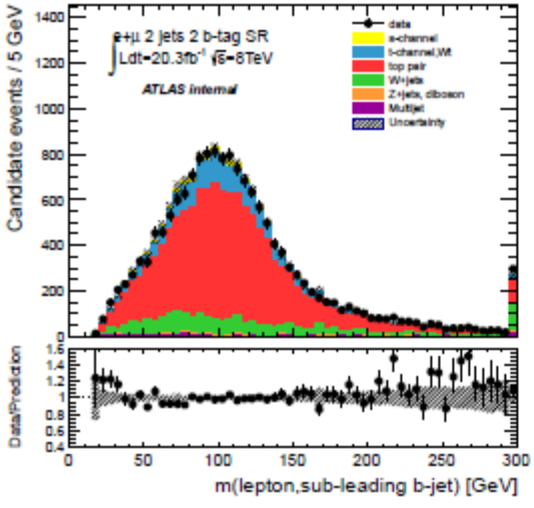

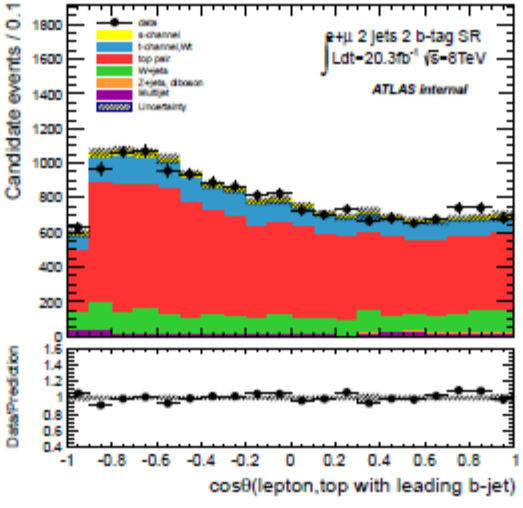

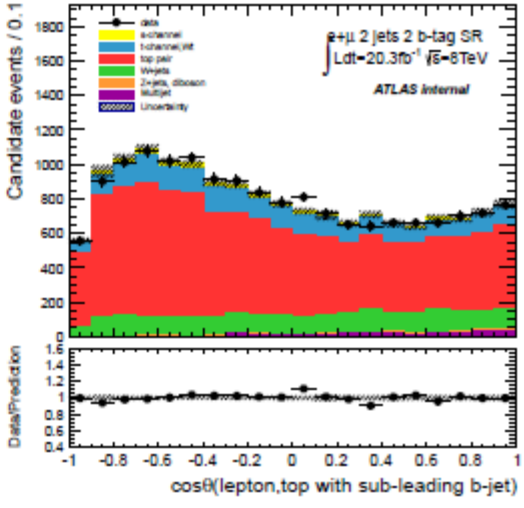

8 TeV systematic shapes

For which sources of uncertainty the shape variations need to be considered?

1) Kolmogorov-Smirnov test for nominal BDT distribution and $\pm 1\sigma$ variation. If KS<0.6, shape uncertainty included in the statistical tool

2) Uncertainties whose KS is within (0.6-0.8) are kept if their effect on the s-channel cross section uncertainty is > than the one of simulation statistics

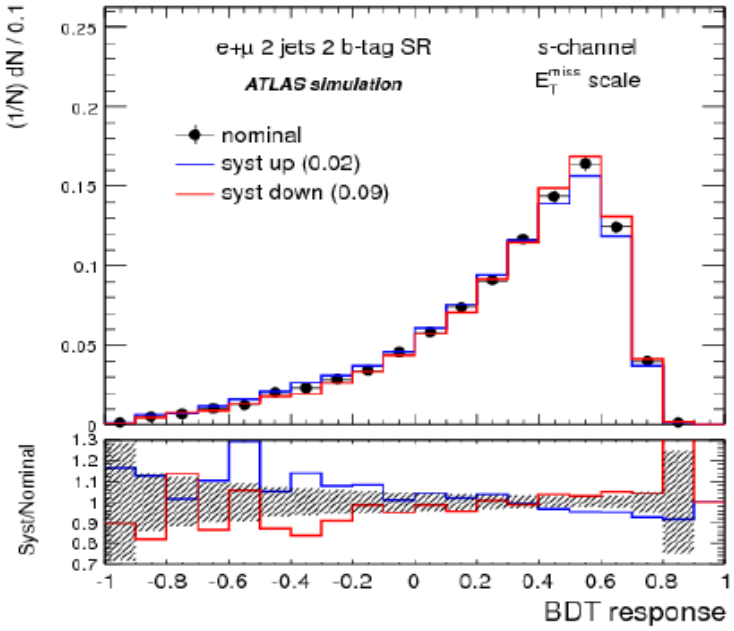

3) Reliability of the criteria 1) & 2) examined by varying the binning of the classifier or by smoothing the distribution of one particular process

8 TeV impact of MET SCALE

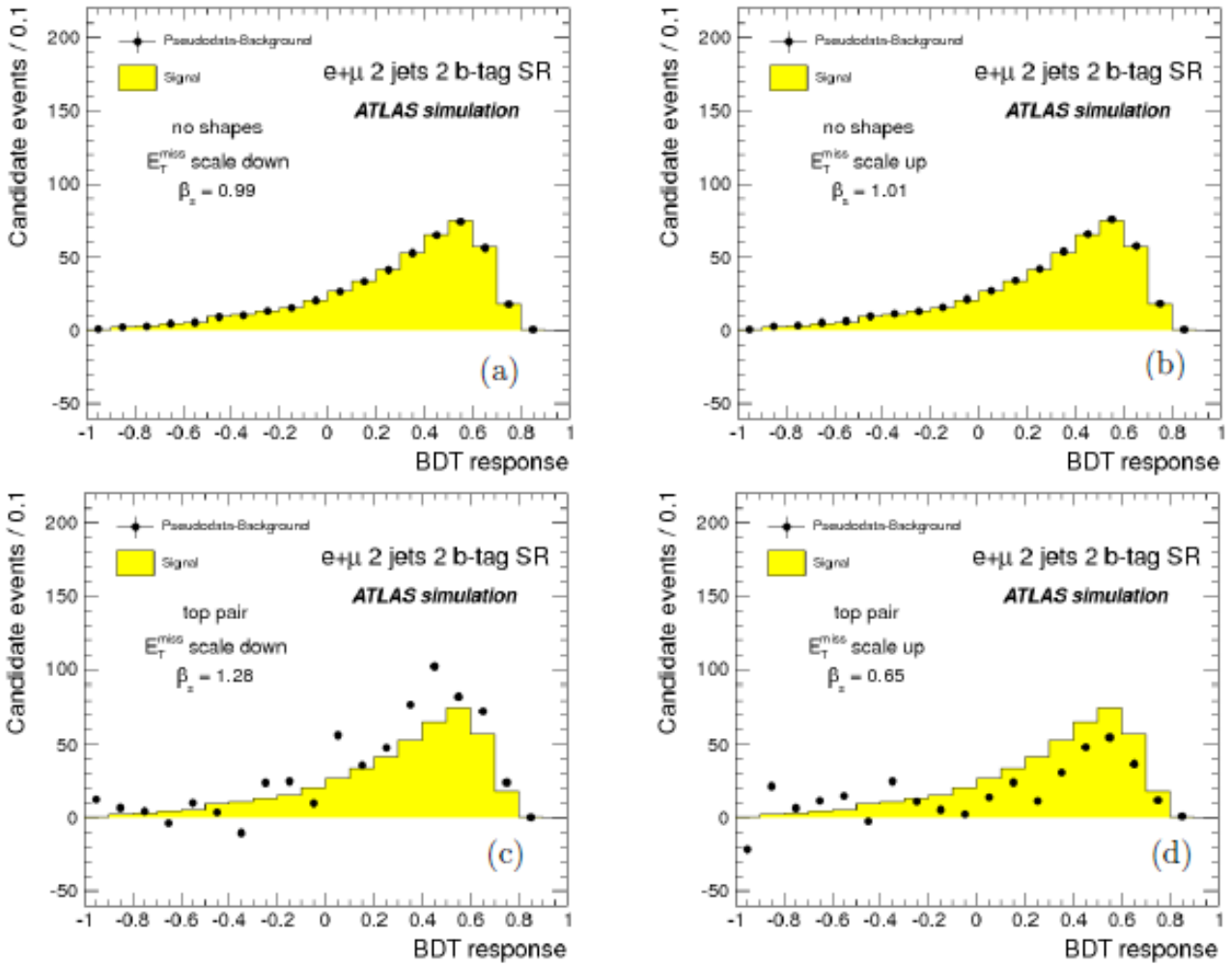

Figure F.3: Expected signal distributions of the BDT classifier after background subtraction to the pseudo-data including the E_T^{miss} scale $\pm 1\sigma$ variations (a) down uncertainty with rates only, (b) up uncertainty with rates only, (c) down uncertainty with $t\bar{t}$ shape and (d) up uncertainty with $t\bar{t}$ shape. The statistical errors of the Monte Carlo signal sample are smaller than the size of the points.

8 TeV impact of JET SCALE

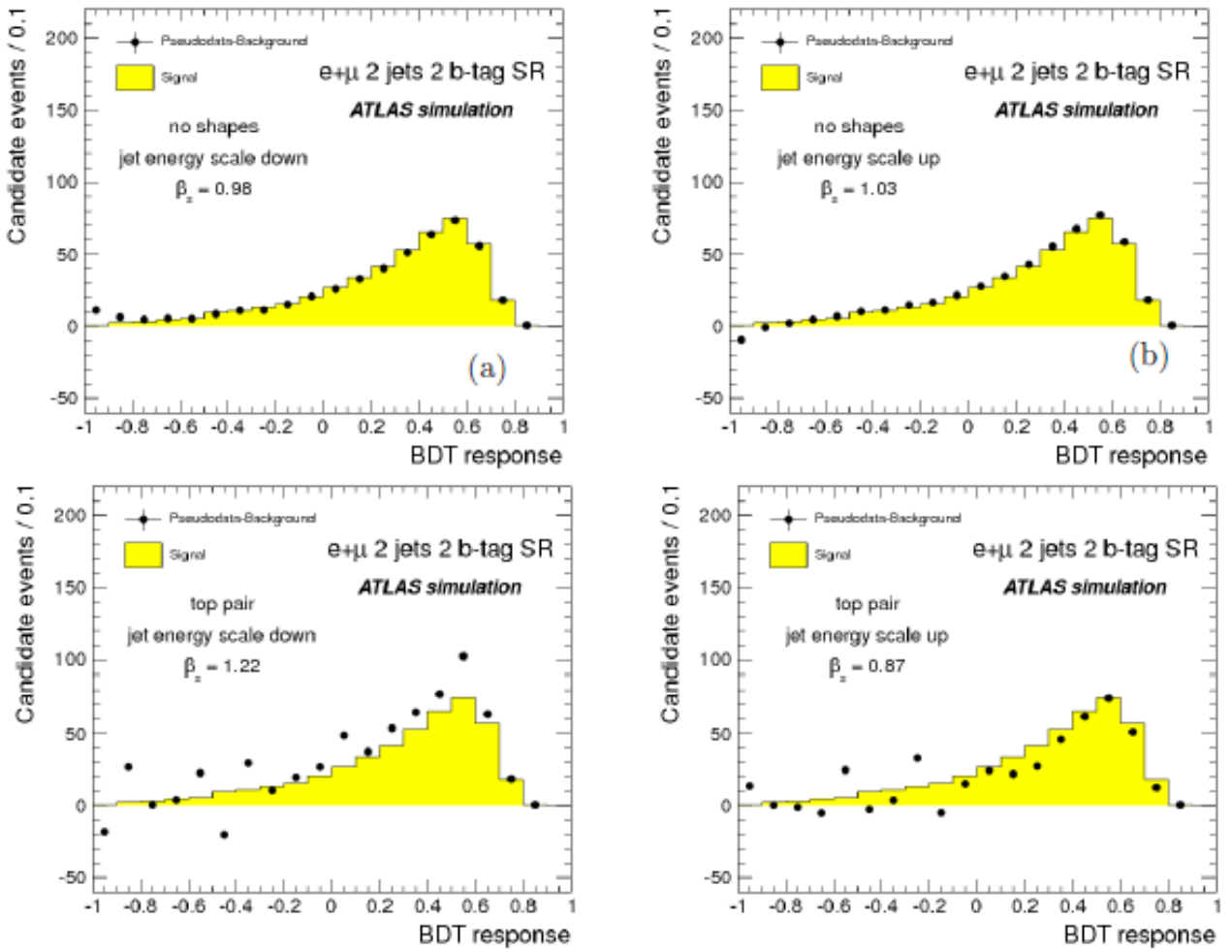

Figure F.4: Expected signal distributions of the BDT classifier after background subtraction to the pseudo-data including the jet energy scale $\pm 1\sigma$ variations (a) down uncertainty with rates only, (b) up uncertainty with down with rates only. (c) down uncertainty with $t\bar{t}$ shape and (d) up uncertainty with $t\bar{t}$ shape. The statistical errors of the Monte Carlo signal sample are smaller than the size of the points.